SAPIENZA
UNIVERSITÀ DI ROMA

DOTTORATO DI RICERCA IN BIOCHIMICA
CICLO XXIV (A.A. 2008-2011)

Role of ERp57 in the regulation of gene expression and its involvement in neurodegeneration

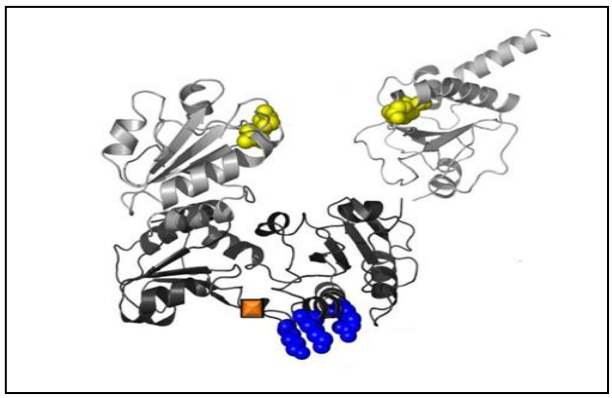

Docenti guida
Prof.ssa Maria D'Erme
Prof.ssa Anna Ferraro

Coordinatore
Prof. Paolo Sarti

Dottoranda
Cristina Aureli

Dicembre 2011

SAPIENZA
UNIVERSITÀ DI ROMA

DOTTORATO DI RICERCA IN BIOCHIMICA
CICLO XXIV (A.A. 2008-2011)

Role of ERp57 in the regulation of gene expression and its involvement in neurodegeneration

Docenti guida
Prof.ssa Maria D'Erme
Prof.ssa Anna Ferraro

Coordinatore
Prof. Paolo Sarti

Dottoranda
Cristina Aureli

Dicembre 2011

Credo di poter affermare che nella ricerca scientifica
né il grado di intelligenza né la capacità di eseguire e portare
a termine il compito intrapreso siano fattori essenziali per la
riuscita e per la soddisfazione personale. Nell'uno e nell'altro
contano maggiormente della totale dedizione e il chiudere gli
occhi davanti alle difficoltà:
in tal modo possiamo affrontare i problemi che altri,
più critici e più acuti, non affronterebbero.

La ricerca << partigiana >>
Rita Levi Montalcini

A Massimiliano

Contents

1 Introduction

1.1 ERp57

The endoplasmic reticulum (ER) serves many general functions, including the facilitation of protein folding and the transport of newly synthesized protein. Moreover, ER has functions in several metabolic processes, such as lipids and steroids synthesis, in protein post-translational modifications, in the regulation of calcium concentration and in modulation of the stress responses. There are ER numerous proteins dealing with these different functions. One of these proteins, ERp57, is an ER luminal glycoprotein specific thiol oxidoreductase that is a member of the protein disulfide isomerase (PDI) family (Freedman et al. 1994).

ERp57 has been referred to as Grp58, ERp60, ERp61, PDI-Q2, PDIA3 and 1,25D3-MARRS (Membrane Associated, Rapid Response Steroid binding).

ERp57 has been most widely studied for its role in the immune system because of its involvement in the heavy chain assembly of major histocompatability complex (MHC) class I molecules (Wearsch and Cresswell 2008). Nevertheless, there is an increasing number and type of functions in which it seems to be involved.

In 1988 the cDNA encoding ERp57 (then referred to as ERp60) was first isolated from numerous animal species and mistakenly identified as phosphoinositide-specific phospholipase C (PI-PC) with surprising amino

acid sequence similarity of ERp60 thioredoxins (Bennett et al. 1988). A decade after this finding, the cDNA encoding human ERp57/Grp58 was cloned independently in three different laboratories (Bourdi et al. 1995; Hirano et al. 1995; Koivunen et al. 1997). All of them reported that the gene encodes a 505-amino acid polypeptide with significant homology to human protein disulfide isomerase.

The sequence includes a putative nuclear localization motif and a endoplasmic reticulum retention/retrieval motif (Bourdi et al. 1995).

The human gene encoding ERp57 consists of 13 exons and 12 introns, spans 18 kb in length and encodes a 505 amino acid protein, that is highly expressed in human liver, lung, placenta, pancreas and kidney; with lowest expression in the heart, skeletal muscle and brain (Koivunen et al. 1997).

1.1.1 Structure

ERp57 has distinct structural and functional domains (Fig. 1).

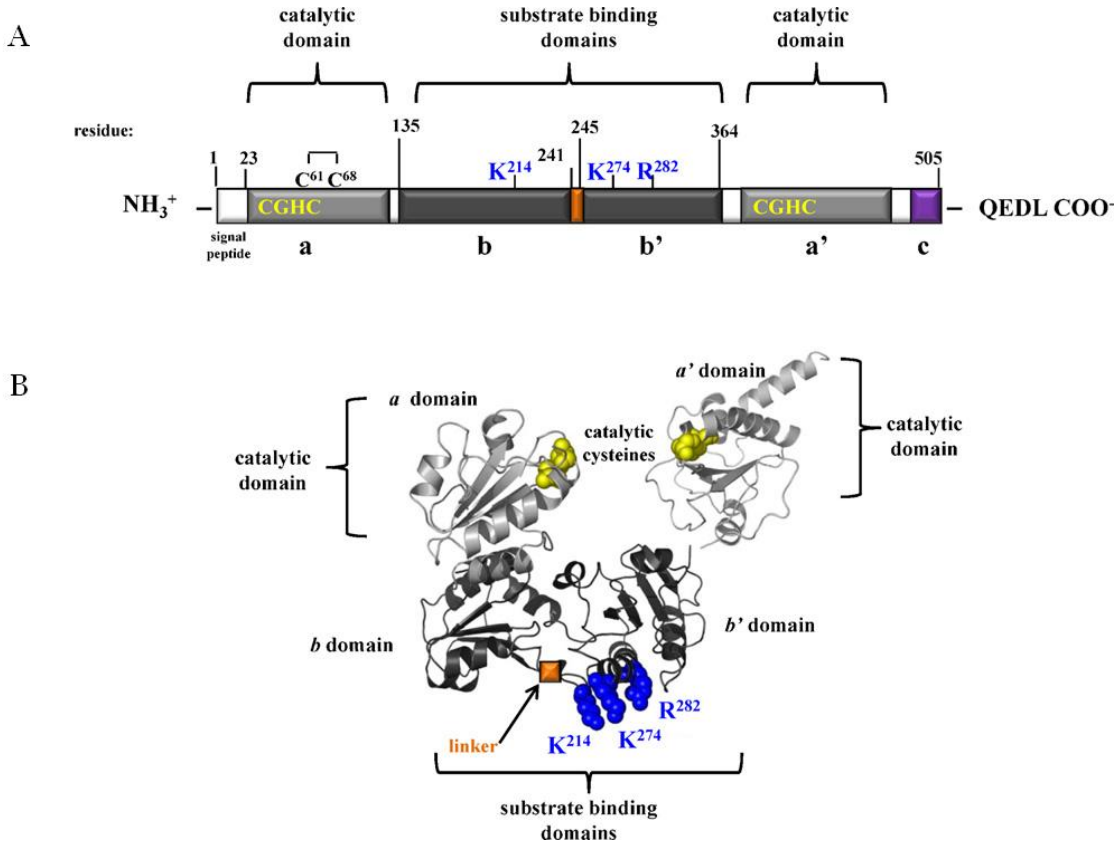

Figure 1. A linear representation of ERp57 and B three-dimensional model of ERp57. The protein contains an N-terminal amino acid signal sequence and a C-terminal QDEL endoplasmic reticulum (ER) retention signal. In both the linear and three-dimensional model, the catalytic a and a' domains are shown in light grey while the substrate binding b and b' domains are shown in dark grey. The yellow amino acids indicate the catalytic residues CGHC and the blue amino acids indicate residues involved in calnexin binding. In the linear model, the short linker between the b and b' domains is marked in orange and the basic C terminal is marked in purple. Three-dimensional model of the a b b' a' domains based on NMR studies of the a and a' domain of protein disulfide isomerase (PDI) (Tian et al. 2006) and the b and b' domains of ERp57 (Kozlov et al. 2006).(Coe and Michalak 2010).

ERp57 has a domain architecture of four thioredoxin-like domains (**a b b' a'**) and is highly similar to PDI in both domain organization and amino acid sequence and sharing with this protein the 33% overall identity (Kozlov et al. 2006). NMR studies have shown that ERp57 adopts an overall U shape similar to that of PDI with the catalytic sites of the two active thioredoxin domains facing each other.

The ERp57 **a** and **a'** domains are highly similar to PDI sharing 50% amino acid identity in these catalytically active CGHC motif domains. Both **a** and **a'** domains show characteristic features of folded proteins, having both α strands and β sheets with no noticeable differences in the secondary structure when oxidized or reduced a' domain are compared. The a domain, containing a structural disulfide bond formed between two cysteines (Cys61 and Cys68), presents only minor differences in both redox state (Frickel et al. 2004).

The redox potentials of the of ERp57 **a** and **a'** domains are −0.167V and −0.156 V, respectively, and these potentials are comparable to the redox potential of PDI (−0.175 V). The disulfide reductase and isomerase activities of the a and a' domains are 20 times lower than those of PDI.

The ERp57 **b** and **b'** domains are two thioredoxin-like domains connected by a short linker. They are critical for binding to the lectin-like ER chaperone calnexin (Kozlov et al., 2006).

The **b** and **b'** domains have approximately 20% amino acid identity to PDI, but the ERp57 b' domain has a long deletion while the b domains of ERp57 has two 6–7 residue inserts; this loop contains residues that are critical for binding to calnexin (Kozlov et al., 2006).

As mentioned before, ERp57 has a ER retrieval sequence (QEDL) in its C-terminal and unlike PDI, does not have an acidic carboxyl terminus but

instead a basic carboxyl terminal domain: this difference modulate the substrate binding specificity (Khanal and Nemere 2007).

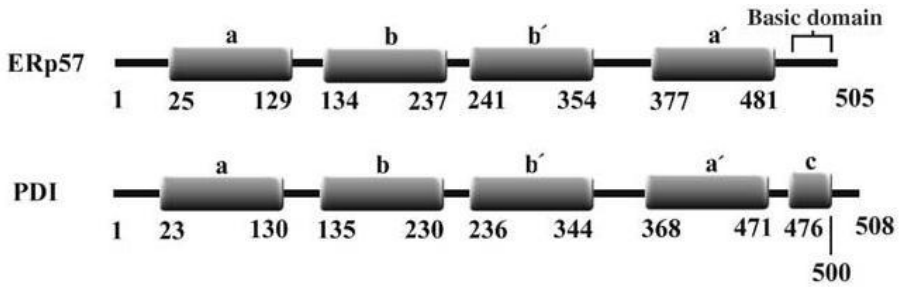

Figure 2. Organization of the a b b' a' domains of ERp57 compared with PDI.
The residue numbers of the individual thioredoxin-like domains are given. The a b b' a' domains of ERp57 and PDI are similar, except that ERp57 has a basic C-terminus and PDI has an acidic c domain.(Pollock et al. 2004)

Interestingly, PDI and ERp57 also show a deep difference in their **b** and **b'** domains surface charges. In fact, there is a formal charge of +4 in the b' ERp57 α2' helix, while in PDI this charge is −4. The positive charge of ERp57 has a role in binding the negative tip of the P-domain of calnexin. When these residues are mutated the binding to calnexin is abrogated. Hence, the **b'** domain is critical for the binding of calnexin, while the **b** domain strengthens this interaction.

1.1.2 Main ERp57 biological functions

ERp57 has been reported to be involved in a variety of cellular functions, summarized in Table 1(reviewed in Turano et al.2011).

Table 1 Localizations, activities and functions of ERp57. (Turano et al. 2011)

Locations	Activity	Function	Ref.
Endoplasmic reticulum	Disulfide isomerase	Folding monoglucosylated proteins	(Oliver et al. 1997; Oliver et al. 1999)
	Disulfide isomerise	Dissociation of the capsid proteins of SV40	(Schelhaas et al. 2007)
	Disulfide bond formation	Assembly of the major histo-compatibility complex (MHC) class I	(Lindquist et al. 1998)
	Redox activity	Redox state of the sulfhydryl groups in the intraluminal portion of SERCA	(Li and Camacho 2004)
	Interaction with the all-trans retinoic acid receptor α	Submit the receptor to the degradation process known as ERAD	(Zhu et al. 2010)
	Interaction with STAT3, in mouse embryonic fibroblasts	Modulation of STAT3 signaling from the lumen of the endoplasmic reticulum	(Coe et al. 2010)
Cell surface	Interaction with calcitriol	Fast activation of non-genomic processes of calcitriol (involving PLA2; PKC; ERK) Stimulation of phosphate uptake. Internalization and nuclear import	(Nemere et al. 2004) (Boyan et al. 2007; Tunsophon and Nemere 2010) (Wu et al. 2010)
		Regulation of bone-related gene transcription and mineralization in osteoblast-like MC3T3-E1 cells	(Chen et al. 2010)
	Interaction with the		(Mah et al. 1992)

	angiotensin II receptor		
	Interaction with vasopressin receptor		(Aiyar et al. 1989)
	Interaction with the all-trans retinoic acid receptor α		(Zhu et al. 2010)
	Interaction with STAT3 in the lipid raft fraction of cell membrane	Participation of a signal transduction pathway initiating at the cell surface	(Sehgal et al. 2002) (Guo et al. 2002)
Cytosol	Interaction with STAT3 in the cytosol	Present in a multiprotein complex	(Ndubuisi et al. 1999) (Guo et al. 2002)
	Interaction with the all-trans retinoic acid receptor α	Transport of the ligand-receptor complex into the nucleus (in the Sertoli cells)	(Zhu et al. 2010)
	Interaction with NFκB in the cytosol of leukemic cells		(Wu et al. 2010)
	Redox activity; interaction with Ref-1	Maintenance of the reduced state of Ref-1 (complex, shuttles between the cytosol and the nucleus)	(Grillo et al. 2006)
	Interaction with mTOR	Assembly and functioning of the multiprotein complex mTORC1; Appears to be at least in part responsible for the redox dependence of mTORC1 activity	(Ramirez-Rangel et al.)
Nucleus	Redox activity; interaction with Ref-1	Maintenance of the reduced state of Ref-1 (complex, shuttles between the cytosol and the nucleus)	(Grillo et al. 2006)
	Interaction with STAT3	Binding to enhancers, known to bind STAT3 for the activation of the corresponding genes; involvement in the signaling and/or DNA binding of STAT3	(Chichiarelli et al. 2007)
	Protein complex with HMGB1, HMGB2, HSC70, glyceraldehyde 3-phosphate dehydrogenase and ERp57	Recognition of the incorporation of the modified nucleosides into the DNA (resulting in genotoxic stress, eventually leading to apoptosis); ERp57 is essential for the phosphorylation of histone H2AX	(Krynetski et al. 2003) (Krynetskaia et al. 2009)

	Interaction with Ku80, Ku70 and nuclear matrix protein 200/hPso4	Participation in more than one process of DNA repair (unknown mechanism)	(Grillo et al. 2006)
	Presence in multimeric nuclear complexes, containing nucleophosmin, nucleolin, TUBB3 (a specific isotype of tubulin) and β-actin	The interaction appeared to be correlated with paclitaxel resistance	(Chichiarelli et al. 2007) (Schultz-Norton et al. 2006)
	Interaction with A/T rich regions, and in general with MARs (nuclear matrix associated regions) of DNA; Binding requires the oxidized form of ERp57		(Grillo et al. 2007) (Coppari et al. 2002)
	Redox activity on transcription factor E2A (stabilized by disulfide bonds)	Responsible for the inactivation of the factor by reducing its disulfide bonds	(Markus and Benezra 1999)
Mitochondria	Interaction with calpain	Stabilize calpain, contrasting with its degradation by other mitochondrial proteases; ERp57-calpain complex-catalyzed partial hydrolysis of AIF	(Ozaki et al. 2008)

1.1.3 ERp57 as a member of the chaperone system

The first well characterized function of this thiol-disulfide oxidoreductase in the ER is the one typical of the chaperone proteins.

For recently synthesized glycoproteins, the ER possesses a specific maturation system designed to assist in folding, thereby ensuring the quality of the final products before they are released.

Proteins that are not properly folded are sent to proteosomes for degradation. The molecular components of this folding system are usually referred to as "chaperones".

Being a member of the thiol oxidoreductase family of proteins that facilitate the oxidative folding of glycoproteins (Urade et al. 2004), it catalyzes disulphide bond exchange in substrates that are bound to calreticulin (CRT) or calnexin (CXN) (Martin et al. 2006).

ERp57 interacts specifically with N-glucosylated integral membrane proteins and substrate selection is dependent upon its formation of discrete complexes with soluble CRT or membrane bound CXN (Zapun et al. 1998).

It has been suggested that calnexin or calreticulin has a role in bringing ERp57 and substrate into close proximity, increasing their local concentration, resulting in an apparent enhanced activity of ERp57 (Leach et al. 2002).

The process requires the intermediate formation of a mixed disulfide between the glycoprotein and the proximal cysteine of one of the two active sites of ERp57in oxidation, reduction and isomerisation reactions (Leach et al. 2002).

1.1.4 ERp57 in immune function: MHC class I molecules

One of the most widely studied function of ERp57 is its role in the immune system.

The function of the major histocompatibility complex (MHC) class I molecules is to present cytoplasmatically derived short peptides to cytotoxic T lymphocytes, which can potentially trigger a cascade of immune responses (Pamer and Cresswell 1998). Extracellular pathogens are initially endocytosed and degraded by the proteasome. These peptides are then traslocated in to the ER lumen through a well described pathway, the TAP system. Once within the ER, they are presented to the nascent MHC class I and if the pocket on this protein is complementary, it binds it. The complex is then translocated to the plasma membrane where it presents the bound peptide to the various immunoreactive cells.

In studying MHC class I production, interactions with chaperones were identified. The first of these proteins to be identified in association with the MHC class I heavy chain was calnexin (CXN) (Degen and Williams 1991), which ERp57 requires for its recruitment to heavy chain in the ER. In the early stage, the glycosylated heavy chain binds to both calnexin and ERp57, and this complex catalyzes disulfide bond formation in the heavy chain, allowing it to assemble with the soluble subunit β2-microglobulin. At the late stage, these heterodimers acquire peptides, thus entering the peptide loading complex (PLC) which consists of calreticulin; ERp57; a peptide transporter (TAP) and tapasin, a glycoprotein critical for loading MHC class I molecules with high affinity peptides. Peptides are then loaded in the ER and the heavy chain β2-microglobulin heterodimer dissociates from the PLC and is exported to the cell surface (Zhang et al. 2009).

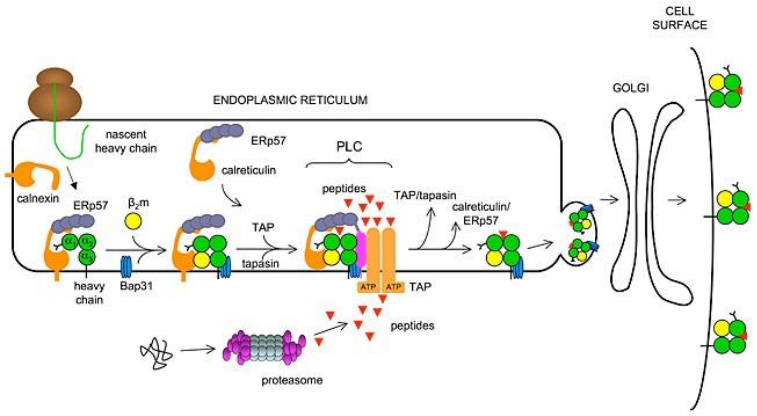

Figure 3. Within the ER, newly synthesized H chains (green) associate with the membrane-bound molecular chaperone calnexin (orange) and ERp57 (purple). The calnexin-H chain complex then binds to the β-2m subunit (green). At this point, calnexin may remain or it may be replaced by its soluble homolog calreticulin . Yet another protein, Bap31 (blue), binds at this stage. Subsequent association with the TAP transporter (orange) occurs in an interaction that is bridged by tapasin (pink). This multi-subunit complex consisting of calnexin (or calreticulin), H chain, β-2m, tapasin, TAP, ERp57 and Bap31 is known as the "peptide-loading complex" or PLC. Following peptide binding to class I, the peptide loading complex dissociates and the fully assembled class I molecule is exported to the cell surface. Once at the cell surface, peptide-class I complexes are scrutinized by T cell receptors on circulating cytotoxic T cells. If the T cell receptor binds with sufficiently high affinity, the infected cell will be killed.

The centrality of ERp57 in antigen processing is underscored by the impaired assembly of the MHC class I peptide-loading complex in mice deficient in it and the embryonic death of all 64 mouse embryos thath were exposed to ubiquitous deletion of the protein (Garbi et al. 2006).

1.1.5 ERp57 as membrane associated receptor

An unexpected function of ERp57 on the cell surface is the binding of the hydroxylated, hormonal form of vitamin D3, i.e. 1α,25-dihydroxycholecalciferol (1α,25-$(OH)_2D_3$, calcitriol) (Nemere et al. 2004), followed by fast activation of non-genomic processes and the internalization and nuclear import of ERp57 itself. This finding was the consequence of a search for a membrane receptor, whose existence was established by ligand binding studies. Rapid responses are not expected to be the result of the involvement of the classical vitamin D receptor (VDR), which operates through binding to DNA and the activation of gene expression, and therefore requires longer times to produce detectable events. The rapid cell response (seconds or minutes) after stimulation with 1α,25-$(OH)_2D_3$ activates numerous cascades of signal transduction, involving signaling proteins such as phospholipases C (PLC) and A2 (PLA2), protein kinases C (PKC) and ERK (extracellular response activated kinase), all of which have been shown to respond to the formation of the ERp57-1α,25-$(OH)_2D_3$ complex (Chen et al. 2010).

ERp57 is also important for the steroid hormone-stimulated calcium uptake in mammalian intestinal cells (Nemere et al. 2010). ERp57 modulates the vitamin D-mediated anti-cancer activity, specifically in breast cancer.

1,25$(OH)_2D_3$ stimulates PLA2-dependent rapid release of prostaglandin E2 (PGE2), activation of protein kinase C (PKC), and regulation of bone-related gene transcription and mineralization in osteoblast-like MC3T3-E1 cells via a mechanism involving ERp57 (Chen et al. 2010). These data suggest that ERp57 is an important initiator of 1,25$(OH)_2D_3$-

stimulated membrane signaling pathways, which have both genomic and non-genomic effects during osteoblast maturation (Chen et al. 2010).

1.1.6 ERp57 as a stress-response protein

ERp57 has been initially identified as a protein overexpressed in K12 cells, subjected to a stress caused by glucose depletion. This overexpression response has subsequently been confirmed in many cell types and with different stress inducing agents (Murray et al. 2004).

The chaperone and redox activities of overexpressed ERp57 are expected to counteract some deleterious effects of cell stress, such as protein misfolding or damage caused by reactive oxygen species, and a number of studies have confirmed this behavior, although they have also revealed great differences in the response and in the protection provided, depending on the type of stress and on the cells which were examined.

In some cases the knowledge of these effects might even be exploited for a therapeutic intervention, as proposed in a recent study (Corazzari et al. 2007), in which the mechanism of action of antitumoral agents was investigated.

A further example of cell-protecting activity of ERp57 emerged from the study of the neurodegenerative disease.

Neurodegenerative disorders such as Alzheimer's disease (AD), Parkinson's disease (PD), Huntington's disease (HD), amyotrophic lateral sclerosis (ALS) and prion protein diseases all share a common feature: the accumulation and aggregation of misfolded proteins (Rao and Bredesen

2004). The presence of misfolded proteins elicits cellular responses that include an endoplasmic reticulum (ER) stress response that may protect cells against the toxic buildup of misfolded proteins.

Accumulation of these proteins in excessive amounts, however, overwhelms the 'cellular quality control' system and impairs the protective mechanisms designed to promote correct folding and degrade faulty proteins, ultimately leading to organelle dysfunction and cell death. The accumulation of misfolded proteins seen in various neurodegenerative diseases leads to an ER stress response.

In light of this considerations, is not surprising the involvement of the protein ERp57 in numerous human disease states such as cancer, prion disorders, Alzheimer's and Parkinson's diseases and ALS (Erickson et al. 2005; Hetz et al. 2005; Tourkova et al. 2005; Nardo et al. 2011; Wilhelmus et al. 2011).

Expression of ERp57 is increased in transformed cells, and it is also thought that the role it plays in oncogenic transformation is directly due to its ability to control intracellular and extracellular redox activities through its thiol-dependent reductase activity (Hirano et al. 1995). Additionally, the role ERp57 in the modulation of STAT3 signalling and proliferation could be exploited and contribute to a cancerous diseased state (Coe et al. 2009).

An increase in ERp57 expression has also been observed in the early stages of prion disease, suggesting that it may play a neuroprotective role in the cellular response to prion infection (Hetz et al. 2005). ERp57 and prion protein interact and this interaction is enhanced in prion infected mouse scrapies.

Erickson et al. (2005) demonstrated that in Alzheimer's disease, ERp57 and calreticulin are carrier proteins that prevent the aggregation of β-

amyloids, a major component of the toxic plaques found in Alzheimer patients.

In PD brain, the tissue transglutaminase enzyme, that catalyzes molecular protein cross-linking and is present in a granular distribution patter, induces cross-links in α-synuclein monomers, oligomers and α-synuclein aggregates. Apart from tTG, these granules were also positive for the protein disulphide isomerase, ERp57 and calreticulin (Wilhelmus et al. 2011).

Furthermore, impaired function because of oxidative/nitrosative modifications of PDI or increased expression of ERp57 in neuronal cells cultured in the presence of the dopaminergic neurotoxin 6-hydroxydopamine has been described (Holtz and O'Malley 2003; Kim-Han and O'Malley 2007).

In summary, these studies implicate ERp57 as a marker of various disease states and demonstrate the importance of ERp57 as a target for developing novel strategies for treatment and early diagnosis of diseases.

1.1.7 Nuclear ERp57 and DNA binding

As aforementioned, ERp57 is localized predominantly in the ER, but also present in cell surface and in cytoplasm. An interesting and least known feature of Erp57 is its localization and its role in the nucleus(Chichiarelli et al. 2007). Indeed, ERp57 has a putative nuclear localization signal in its C-terminus that allows the translocation of the protein disulfide isomerase to the nucleus. ERp57 is associated with scaffold/matrix associated region (S/MAR)-like sequences of DNA (Coppari et al. 2002), and in melanoma M14 cells, ERp57 associated with signal transducer and activator of transcription 3 (STAT3) in the nucleus (Eufemi et al. 2004). Several studies have also shown that ERp57 sequesters both inactive and active STAT3, and may play a role in the regulation of STAT3 signaling (Coppari et al. 2002; Eufemi et al. 2004).

ERp57 has unidentified functions in the nucleus, likely having pleiotropic effects on gene expression. By extension, dysregulation of ERp57 signaling in the nucleus may contribute to hepatocellular carcinoma (HCC) (Grindel et al. 2011).

ERp57 has a Rel homology binding domain (Khanal and Nemere 2007), therefore, NF-kB could provide a carrier shuttle for ERp57 nuclear translocation. It was shown recently that ERp57 can associate with the transcription factor nuclear factor kB (NF-kB) in NB4 promyelocytic leukemia cells (Wu et al. 2010).

2 Preamble

This work intends to investigate the role of the ERp57 protein in two different contexts: i) as protein involved in gene expression regulation, ii) as stress response protein.

In the nucleus, ERp57 is able to bind *in vivo* specific DNA intronic sequences having the features of regulatory regions. Based on this evidence, experiments have been devoted to demonstrate its involvement in the control of gene expression.

The redox changes in the ER are integral parts of the neurodegenerative patho-mechanisms, either as causative agents, or as complications. Recent findings strongly support a role of ERp57 protein in different neurodegenerative diseases such as Alzheimer and Parkinson's diseases. Kim-Han et al. (2007) point out that a mimetic parkinsonian neurotoxin 6-OH-dopamine leads to the rapid formation of high-molecular-weight species of ERp57 and mitochondrial DNA in a dose and time-dependent fashion. Therefore, the stress condition induced by a new endogenous neurotoxin 5-S-Cysteinyldopamine (CysDA), has been evidenced by oxidative stress markers such as protein carbonylation and glutathione levels. Considering the oxidative stress exerted by CysDA, its effects on the distribution and expression of a stress response protein as ERp57 was evaluated.

3 Aim of the work I

The idea of a nuclear localization of ERp57 was at first not easily accepted, not only because the escape of a protein, provided with an ER retention signal, from the endoplasmic reticulum was considered unlikely, but also because of the endoplasmic reticulum shares its membrane with the nucleus.

The first evidence of the nuclear presence of ERp57 emerged from immunofluorescence detection in 3T3 cells and rat spermatids (Ohtani et al. 1993) and from a proteomic study of chicken hepatocytes nuclei, where ERp57 was mainly found localized in the internal nuclear matrix fraction (Altieri et al. 1993).

Subsequently, the presence of ERp57 was demonstrated in the internal nuclear matrix obtained from 3T3 and HeLa cells. Futher evidences indicating Erp57 nuclear localization was obtained from data showing the protein associated to DNA cross-linked with cis-diamminedichloroplatinum II (cis-DDP) or formaldehyde (Coppari et al. 2002).

Moreover, Markus and Benezra have highlighted a regulatory activity of ERp57 on the redox state and functional properties of the E2A

transcription factor, hypothesizing a role for ERp57, as modulator of trascription factors (Markus and Benezra 1999).

The findings by Krynetski and coworkers (Krynetski et al. 2003) demonstrated that ERp57 was present in a multiprotein complex responsible for recognition of DNA damage in cells with an inactive mismatch repair system. This hypothesis has been further corroborated by the association with the human apurinic/apyrimidinic endonuclease (APE/Ref-1) (Grillo et al. 2006), a dual-function protein that has important roles in the repair of baseless sites that arise in DNA and in regulating the redox state of several proteins (Yacoub et al. 1997).

Previous data obtained in our lab, have demonstrated that ERp57 was able to interact with MSH6, TMEM126A and Ets-1 gene sequences in HeLa cells (Chichiarelli et al. 2007) and in melanoma cell line (M14) cells by ChIP assay (Aureli et al., 2011 submitted). In particular, MSH6 (muts homolog6 (E. coli) gene sequence is the fourth intron of the gene located on chromosome 2; it is involved together with MSH2, in the repair of base substitutions and small mismatched loops (Martin et al. 2010). The second gene sequence of interest, TMEM126A is a portion of the 5' region of the gene TMEM126A, strongly expressed in the brain, which encodes for mitochondria-localized mRNA (MLR) proteins and may be essential in the early nucleation process of large mitochondrial complexes (Hanein et al.

2009). Ets-1 (E26 transformation-specific sequence) gene sequence is an intron of Ets-1 gene and it is a member of the Ets family transcription factors that play many roles in different biological processes such as cell growth and survival (Hanein et al. 2009). Moreover, it has been demonstrated that Ets-1 is implicated in melanoma cells protection under ER stress-induced apoptosis (Dong et al. 2011).

The following actions were taken to get more insight into the role of ERp57 in gene expression regulation:

- MSH6, TMEM126A and Ets-1 chromatin regions were analyzed for their sensitivity to DNase I digestion.
- The influence of ERp57 on MSH6, TMEM126A and Ets-1 gene expression was evaluate by RNA interference strategy and subsequent Real-Time PCR analyses
- To assess the interaction of MSH6, TMEM126A and Ets-1 with ERp57 and its potentially related proteins *in vitro* binding assay were performed.

4 Materials and Methods I

4.1 Cell Culture

Human melanoma (M14) cells were grown to 70-80% confluence at 37°C and in an atmosphere of 5% CO_2 in RPMI 1640 medium, supplemented with 10% fetal bovine serum, 1% w/v sodium pyruvate, 2mM glutamine, 100 U/ml of penicillin and 100 µg/ml of streptomycin.

4.2 Detection of DNase I hypersensitivity

Nuclei from M14 cells were purified as previously described by Chichiarelli et al., 2007. Briefly, M14 cells were manually scraped and washed three times with PBS by centrifuging 5 min at 1,500g. Cells were lysed in lysis buffer (50 mM Tris-HCl pH 7.9, 100 mM KCl, 5 mM $MgCl_2$, 0.025% Triton X-100, 50% 1 g Glycerol, 200 mM β-mercaptoethanol, 0.15 mM spermine, 0.5 mM spermidine), supplemented with the inhibitor cocktail, by incubation on ice for 15 min, and were then centrifuged for 15 min at 1,300g. The pellet was resuspended in Buffer A (50 mM Tris-HCl pH 7.9, 100 mM NaCl, 3 mM $MgCl_2$, 1 mM DTT, 0.2 mM PMSF, 0.15 mM spermine, 0.5 mM spermidine) and centrifuged 15 min at 1,300g. The

purified nuclei were stored at -80°C in Buffer A (0.25 mg DNA/ml). The whole procedure was performed at 4°C.

The DNase I hypersensitivity assay was performed as described by Sambrook and Russel (2001) by treating the nuclei at 37°C for 20 min with different amounts of DNase I; 0.0625U/µl (1/160) and 0.015625U/µl (1/640), respectively. The DNA hypersensitive regions were identified according to Feng and Villeponteau (1992) by means of a semi-quantitative PCR analysis. The PCR amplification of the different clones was performed amplifying each clone PCR with JumpstartREDAccuTaq (Sigma) and a Perkin Elmer thermal Cycler 2400, using the program steps showed in Table2. The obtained PCR samples were subjected to 2% agarose gel electrophoresis.

Table 2. Program steps for PCR amplification of the different clones

Denaturation	96°C	60 sec
Cycle 1-25:		
Denaturation	94°C	15 sec
Annealing	57°C	30 sec
Extension	68°C	2 min
Final extension	68°C	10 min

The method was tested on two well-characterized sequences present in the 5'-region of the MYC gene (Mautner et al., 1995). One, here indicated as Myc-2, is known to be DNase hypersensitive (NC_000008, from 128820577 to 128821252), the other, here indicated as Myc-3, is known to be DNase resistant (NC_000008, from 128811402 to 128811787). The best reproducible results were obtained when the DNA remaining intact after a

digestion with 5 U/ml of DNase I was compared to that remaining intact with 1.25 U/ml of DNase I. In the latter condition the initial fragmentation of DNA favored a complete recovery of the DNA subjected to purification and amplification.

The analysis of DNase I hypersensitivity was carried out in more detail using three couples of primers: MSH6, TMEM126A and Ets-1 (Table 3).

Table 3. couples of primers for PCR amplification

	Left Primer	**Right Primer**
Myc2	5'-TCATACACCTCTGAAACCTTGG-3'	5'-TAATGAGGCTTTGGACACACC-3'
Myc3	5'-ATAGCAGAGACAGGCCAGTGA-3'	5'-TTCCCCTCCTGGCTTTTAGTA-3'
MSH6	5'-GTTGCCCAGGCTAGAATATG-3'	5'-AGAGGCTGACACGAGAGGTC-3'
TMEM126A	5'-AGAGGAGAGCATAAGGTACTGGT-3'	5'-CTTGGAAGAGCTCTGAGAGATAGG-3'
Ets-1	5'-TGGATACTGCTAGGGCCAAC-3'	5'-GGATAGGGGAGGAGTCAAGG-3'

4.3 ERp57 siRNA silencing

The silencing of the protein ERp57 in M14 cells was obtained by the administration of specific siRNA (Hs_GRP58_6_HP Validated siRNA, QIAGEN). The day before transfection, 2.5 x 104 cells per well of a 96-well plate in 100 µl of a complete culture medium (containing serum and antibiotics) were seeded. The cell cultures were grown under normal growth conditions. The siRNA was used at 0.3 µg/µl final concentration and LipofectamineTM RNAiMAX (Invitrogen) was used as transfection agent.

The transfection was carried out according to the manufacturer's instructions. M14 cells were incubated with the transfection complexes under their normal growth conditions and gene expression was monitored at the mRNA or protein level after 48 hours. In the gene expression experiments,

cells treated with scrambled, non-specific siRNA duplex (AllStars Negative control siRNA from QIAGEN) were used as control reference to exclude any nonspecific effect due to the treatment.

4.3.1 Total RNA extraction and cDNA synthesis

Cells were harvested and total RNA was isolated with TRIzol Reagent (Invitrogen) following the manufacturer's instructions. RNA was precipitated by adding isopropanol, washed with 75% ethanol and dried air. The total RNA was resuspended in sterile RNase-free water and subjected to reverse transcription.

The reverse transcription of total RNA was conducted with SideStep™ II QPCR cDNA Synthesis Kit (Stratagene), according to the manufacturer's instructions. The reaction was performed with a Perkin Elmer thermal Cycler 2400.

4.3.2 Real-Time PCR

ERp57, MSH6, TMEM126A, Est1 cDNA expression was evaluated with specific primers (QuantiTect® QIAGEN) by Real-Time PCR (RT-PCR), which was performed using a MJ MiniOpticon Detection System (BioRad Laboratories, Ltd) by means of Brilliant® SYBR® Green QPCR Master Mix (Stratagene) and according the following steps: denaturation (95°C for 5 min), amplification repeated 40 times (95°C for 30 s, 55°C for 30 s, 72°C for

30 s). A melting curve analysis was performed following every run to ensure a single amplified product for every reaction. PCR fluorophore acquisition temperatures were set from 40°C to 95°C, reading every 0.5°C.

All reactions were carried out in at least duplicate. GAPDH (RT2-PCR primers from SuperArray) and RPS27A (QuantiTect® QIAGEN) genes were used as reference for normalization and the relative quantification was analysed using Gene Expression Analysis for iCycler iQ Real Time PCR Detection System Software, Version 1.10 (BioRad Laboratories, Ltd).

4.4 *In vitro* Binding Assay

4.4.1 Nuclei purification and nuclear extracts preparation

Cultured cells were scraped, harvested by centrifugation at 440g for 5 min and washed twice with PBS.

Cells were resuspended in a hypotonic lysis buffer [10 mM Hepes, pH 8, 10 mM KCl, 1.5 mM $MgCl_2$, 30 mM sucrose, 0.5 mM dithiothreitol (DTT), supplemented with an inhibitor cocktail (1 mM phenylmethylsulfonyl fluoride, 10 µM amido-phenylmethyl sulfonyl fluoride; 0.2 mM L-1-chloro-3-(4-tosylamido)-4-phenyl-2-butanone, 0.15 µM aprotinin, 1 µg/ml E 64, 1 µM pepstatin)] by using an hypodermic needle. The suspension was incubated in ice for 10 min and was then centrifuged at 1,400g for 10 min at 4°C. The pellet, that contains the nuclei, was resuspended in lysis buffer and 0.05% Triton X-100 and after incubated in ice for 10 min. The suspension was centrifuged at 1,400g for 10 min and the pellet was washed three times

with lysis buffer with 1 mM $CaCl_2$, by centrifuging each time at 1,400g for 10 min at 4°C.

Nuclear extracts were obtained by treating the purified nuclei in ice for 30 min with EN buffer (20 mM Hepes, pH 7.9; 10 mM KCl; 0.42M NaCl; 20% glycerol and the inhibitor cocktail). After the incubation with EN buffer the suspension was centrifuged at 10,000g for 20 min at 4°C. The supernatant contains the nuclear extract, while the pellet was resuspended again in EN Buffer and was incubated in ice for 30 min. The suspension was centrifuged at 10,000g for 20 min at 4°C and the supernatant, containing the nuclear extract was added to the first supernatant rate.

4.4.2 Amplification of the biotinylated DNA fragments

A biotinylated DNA fragments, corresponding to the genes MSH6, TMEM126A, and Ets-1, were obtained by PCR using the same primers described in table 3.

The amplification of the biotinylated DNA sequence was performed using total DNA from M14 cells (40ng/µl stock solution) and JumpstartREDAccuTaq (Sigma). A Perkin Elmer thermal Cycler 2400 was utilized for the PCR amplification and the protocol used was the following: denaturation (96°C for 1 min), amplification repeated 30 times (94 °C for 15s, 57 °C for 1min, 68 °C for 2mins) and extension (68 °C for 10mins).

The amplification generated a single band displaying the predicted size. The amplified DNA fragments were then purified using a commercial kit (QIAEX® II Gel extraction kit, Qiagen).

4.4.3 Purification of multiprotein complexes by using Dynabeads

Streptavidin-coated magnetic beads (Dynal) were washed three times in buffer A (10 mM Tris–HCl, pH 7.5; 1 mM EDTA, and 2M NaCl, protease inhibitor cocktail) using a magnetic separator (Dynal MPC). The biotinylated DNA fragments, corresponding to the genes MSH6, TMEM126A and Ets-1, were incubated with the beads (50 pmol of DNA for 0.5 mg of beads) for 2 hours at 4 °C in buffer A (Sample). Control experiments were carried out by using streptavidin-beads saturated with biotin in buffer A (Control).

Beads from Sample and Control were then incubated with 10nM biotin in buffer A for 15 min at 4 °C. The beads were isolated using the magnetic separator (Dynal MPC) and washed three times in buffer A. Subsequently the Beads from Sample and Control were incubated with 0.5% BSA in buffer A for 15 min at 4 °C and then were washed three times in buffer A and one time in buffer B (20 mM Tris-HCl pH 8, 5 mM EDTA, 5% glycerol, 0.1% Nonidet P40, protease inhibitor cocktail) using each time the Dynal MPC. The use of the 10nM biotin and of the 0.5% BSA is necessary to block the free streptavidin sites on the magnetic beads.

The nuclear extracts was divided into two equal aliquots and one of these was mixed with DNA-coated beads (Sample), while the other one was mixed with biotin-coated beads (Control). The beads from Sample and Control were then incubated o.n. with gentle agitation at 4°C . The day after the beads were isolated using the Dynal MPC and washed four times in buffer C (20 mM Tris–HCl, pH 8; 5 mM EDTA; 5% glycerol; 0.1% Nonidet P40; 50mM NaCl

and the protease inhibitor cocktail), and once with buffer TE (10 mM Tris–HCl, pH 8 and 1mM EDTA).

The specifically bound proteins were eluted twice with 0,4M NaCl and subsequently twice with SDS buffer (62,5 mM Tris–HCl, pH 6.8; 2% SDS; 10% glycerol; bromophenol blue). In each elution steps the beads were incubated with the elution buffers for 30 min with gentle agitation at room temperature.

The eluted proteins from Sample and Control were analyzed by SDS-PAGE and Western blotting using polyclonal anti-ERp57, anti-Ref1; anti-Parp1 and anti-Ku86 antibodies.

5 Results I

5.1 MSH6 and TMEM126A display DNase I hypersensitive sites

Previous results obtained by Chichiarelli et al (2007) showed the interaction of ERp57 with MSH6, TMEM126A and Ets-1 gene sequences in HeLa and M14 cells. Therefore, DNase I hypersensitivity analyses were carried out to assess whether regulatory regions were localized in these gene sequences.

To this purpose M14 cells nuclei were treated by decreasing concentrations of the enzyme DNase I and the DNA was then extracted and subjected to PCR using specific primers for the three regions of interest. A control sample was subjected to the same procedure without DNase I enzyme.

The validity of the method was initially tested on two sequences located upstream with respect to the promoter of the proto-oncogene c-myc, human gene that regulates the processes of cell differentiation and proliferation. In particular Myc-2 and Myc-3 sequences were considered, since they are respectively hypersensitive and resistant to the action of the enzyme.

As shown in Figure 4, DNase I-hypersensitive sites are present in Myc-2, as expected. Conversely, an increase of amplified Myc-3 DNA was detected at enzyme decreasing concentrations, indicating the presence of sites less sensitive to digestion.

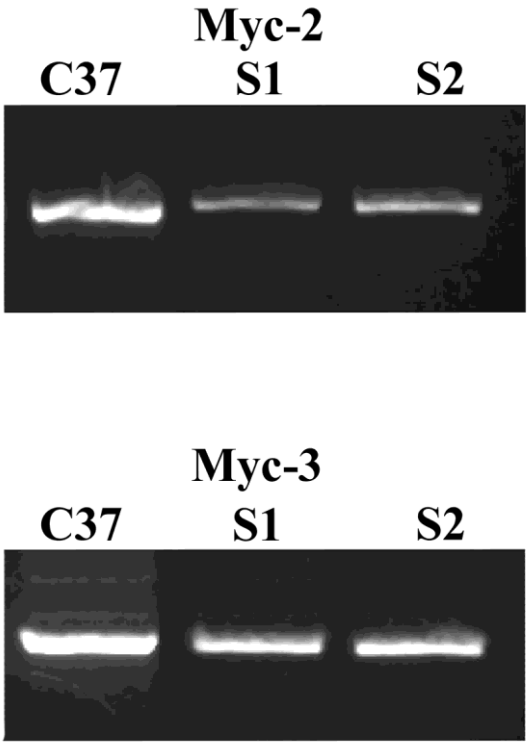

Figure 4: Myc-2 and Myc-3 sequences digested by DNase I. Samples treated with decreasing concentrations of DNase I, 0.0625U/µl (S1) and 0.015625U/µl (S2), respectively or untreated (C37) were analyzed by PCR and subjected to 2% agarose gel electrophoresis.

Once the validity of the method was established, the same procedure was followed to analyze MSH6, TMEM126A and Ets-1 DNA sequences (Fig.5).

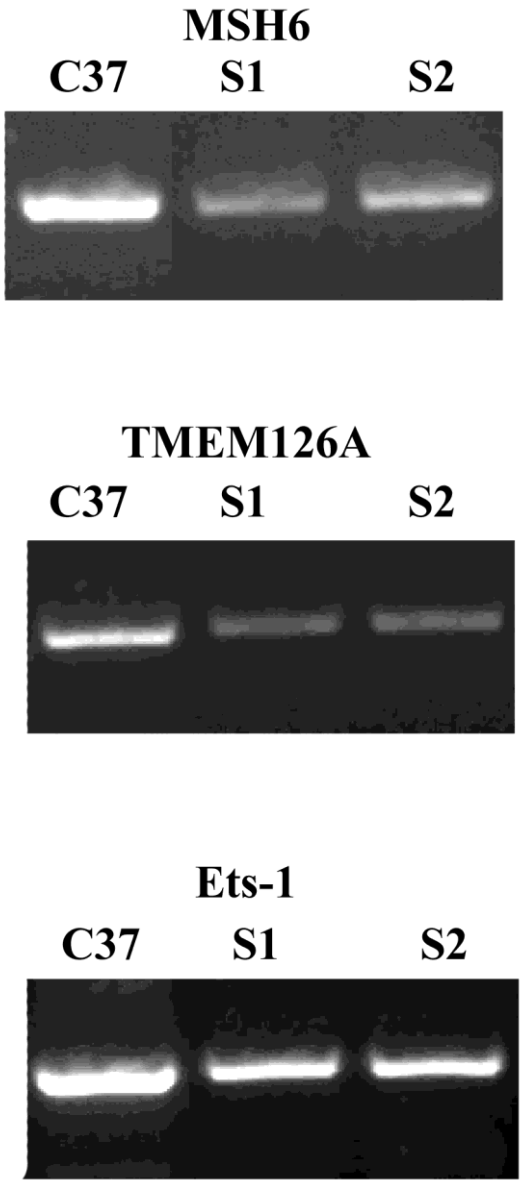

Figure 5: MSH6, TMEM126A and Ets-1.sequences digested by DNase I. Samples treated with decreasing concentrations of DNase I, 0.0625U/µl (S1) and 0.015625U/µl (S2), respectively or untreated (C37) were analyzed by PCR and subjected to 2% agarose gel electrophoresis.

As reported in Figure 6 the densitometric analyses indicate that after DNase I digestion, MSH6 residual DNA was about 30% and 57% at 0,0625U/µl and 0.015625U/µl enzyme concentration, respectively. TMEM126A, was about 19% and 20% at 0,0625U/µl and 0.015625U/µl enzyme concentration, respectively. Conversely, Ets-1 seems unresponsive to the DNase I action, as demonstrated by its 97% and 75% residual DNA obtained at higher and lower enzyme concentration, respectively. The values were normalized to the control sample (C37) and gene sequences are considered hypersensitive when DNA degradation is below 35% compared to the control as indicated by the black line on the graph. Therefore, MSH6 and TMEM126A seem to possess hypersensitivity site.

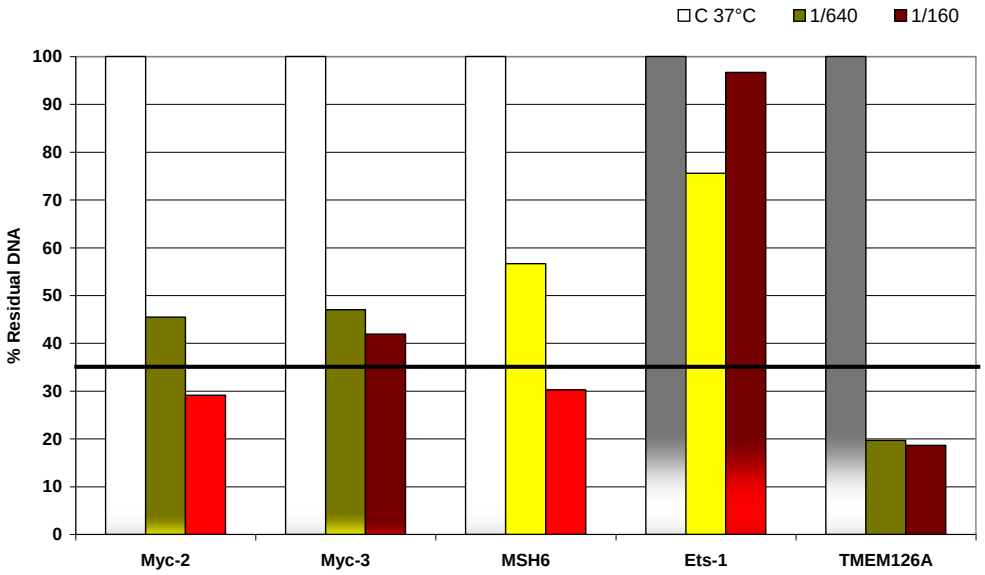

Figure 6. Densitometric analysis of MSH6, TMEM126A and Ets-1 digested by DNase I. M14 cells nuclei were treated or untreated (C37) with decreasing concentrations of the enzyme DNase I, 0.015625U/µl (1/640) and 0.0625U/µl (1/160), respectively. DNA was then extracted and subjected to PCR using specific primers for the regions of Myc-2 and Myc-3. represent positive and negative control of DNase I digestion. The values were normalized against the sample C37 used as control.

5.2 ERp57 siRNA silencing determines a decrease in the MSH6 and TMEM126A genes expression

To verify whether ERp57 is able to modulate MSH6, TMEM126A and Ets-1 genes expression, RNA interfering experiments were carried out using ERp57 short interfering RNA (siRNA).

M14 cells were incubated with specific ERp57 siRNA for 48 hours under normal growth conditions. The silencing of the ERp57 gene and the trascribing activity of its target genes, MSH6, TMEM126A and Ets-1 mRNA were monitored by Real Time-PCR analyses. ERp57 protein silencing was achieved at 48 hours of treatment as demonstrated by Western blotting analysis of M14 cell lysates (data not shown).

The results showed that after 48 hours ,ERp57 mRNA expression was markedly reduced. Due to ERp57 silencing a significant MSH6 and TMEM126A genes expression down-regulation was obtained, whereas the Ets-1 gene was up-regulated, but this effect is not significant due to high standard deviation value gained by the ANOVA test (Fig. 7).

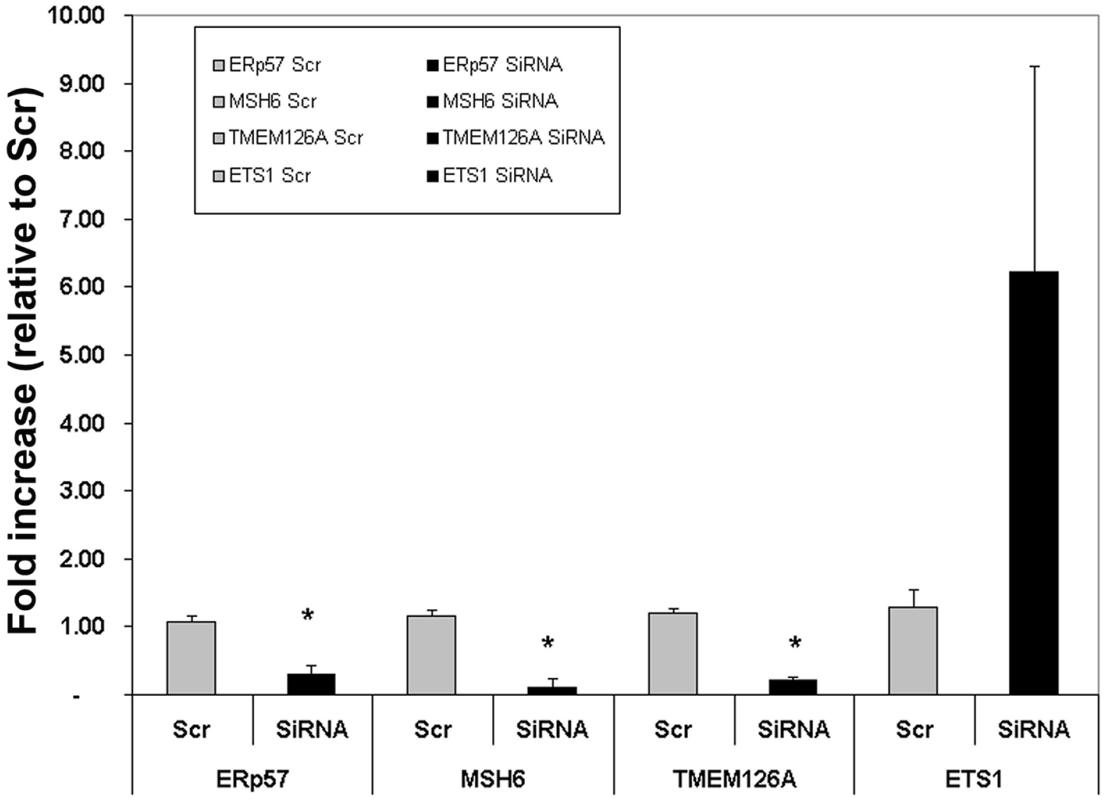

Figure 7. Effect of silencing of ERp57 on the expression of three target genes (MSH6, TMEM126A and Ets-1). M14 cells were treated with the scrambled RNA (Scr) or siRNA for ERp57 (siRNA) and after 48h the total RNA was extracted and determinated by RealTime-PCR. RPS27A (QuantiTect® QIAGEN) gene was used as reference for normalization and fold inductions were calculated using the formula $2^{-(\Delta\Delta Ct)}$. The relative quantification was analyzed using Gene Expression analysis for iCycler iQ real-time PCR detection system software, Version 1.10 (Bio-Rad Laboratories, Ltd.). The values represent the mean ± SD of at least three independent experiments. * $p < 0.05$ vs scrambled cells (Scr).

5.3 *In vitro* binding assay reveals the association of APE/Ref-1 with the ERp57-interacting DNA fragments

To evaluate whether ERp57, Ape/Ref-1(Ref1) and Ku86, both proteins involved in the ERp57 complex formation, or poly(ADP-ribose) polymerase-1 (PARP-1), a protein implicated in chromatin remodeling, were able to bind MSH6, TMEM126A or Ets-1 sequences in M14 cells, DNA binding assay was performed. MSH6, TMEM126A or Ets-1 sequences were biotinylated and immobilized on streptavidin-coated magnetic beads and then incubated with M14 nuclear extracts. The experiments were conducted in the presence of an excess of *E. coli* DNA used as a competitor. Proteins retained by the biotinylated DNA were eluted using a high salt concentration (0.4M NaCl), and then 2% SDS. The samples were subjected to Western blot analyses with Ref1, Ku86 and PARP1 antibodies.

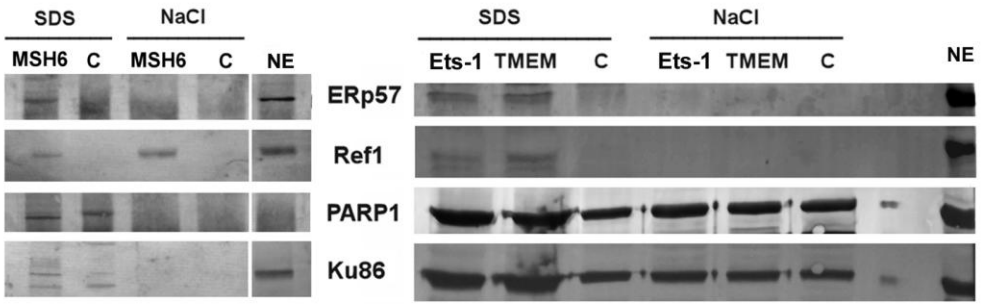

Figure 8. Western blotting analysis with the ERp57, Ref-1, Ku86 and PARP1 antibodies. The samples obtained by the elution of immobilized cloned DNA sequences uncubated with M14 nuclear extract, were probed with the respective antibodies.(C) proteins fron nuclear extract boud to the beads without immobilized DNA regions (NE):represent the 15% of the total nuclear extract. The proteins were eluted with 0.4 M NaCl and then with 2% SDS.

As shown in Fig. 8, Ref1 was associated with the regions of the MSH6, TMEM126A and Ets-1 genes, whereas Ku86 and PARP-1 bound to the genes in unspecific way .

6 Discussion I

Previous results showed that ERp57 binds *in vivo* specific DNA targets, which are mainly present in intronic sequences having the features of regulatory regions. The identification of the DNA sequences bound to the nuclear ERp57 has been demonstrated by ChIP and the cloning procedure of the immunoprecipitated fragments in HeLa cells (Chichiarelli et al., 2007). The features of these DNA sequences, such as the proximity of MAR region and the homology to the non-coding regions of orthologue genes of mouse or rat, are compatible with gene expression regulatory function. Futhermore, ERp57 was also able to bind regulatory regions of several STAT3-dependent genes (Chichiarelli et al., 2010).

Specific genes with high affinity towards ERp57 were selected, from among the ERp57-interacting DNA fragments. In particular, the MSH6 gene which encoded for a DNA mismatch repair protein, the TMEM126A gene which encoded for a recently discovered mitochondrial transmembrane protein and the Ets-1 gene which encoded for a transcription factor and potential oncogene were chosen.

Chromatin digestion by DNase I acts on the nucleosome-free regions of the genome, enabling the identification of both ubiquitous and tissue-specific regulatory elements. Promoters, enhancers, suppressors, insulators, and locus control regions all have been shown to be associated with DNase I hypersensitivity sites (Crawford et al. 2004). Mapping of DNase hypersensitivity sites has also identified a number of inducible gene regulatory elements, such as those associated with genes that are regulated by

steroid hormones or cellular differentiation (Gross and Garrard 1988). Our data show that MSH6 and TMEM126A sequences associated to ERp57, are sensitive to DNase I digestion, supporting the idea of the presence of regulatory regions that could turn on the transcribing process. Conversely, no sensitive site could be identified within Ets-1 sequences-ERp57 associated, suggesting a different function than transcriptional activation for the interaction between the examined Ets-1 region and ERp57.

Previous study has demonstrated the influence of ERp57 in the signaling and transcriptional activities of STAT3 by ERp57 RNA interfering (Eufemi et al. 2004). Our present experiments show that the silencing of ERp57 expression impairs MSH6, TMEM126A activation. Ets-1 is up-regulated, and this effect does not seem to be statistically significant.

Iimportant features of ERp57 are represented by its capacity to function as amolecular chaperone, hence, to interact with several proteins (Quan et al. 1995). In addition, ERp57 could form a multiprotein nuclear complex that preferentially binds DNA with thioguanine incorporated (Krynetski et al. 2003). Grillo et al. (2006) have demonstrated that Erp57 is able to associate with APE/Ref-1, Ku86 in HepG2, Raji and M14 cell lines.

The expression of APE/Ref-1 can be up-regulated by a variety of Reactive Oxygen Species (ROS) and ROS-generating systems (Kelley and Parsons 2001). Interestingly, APE/Ref-1 was recently found to be required for the DNA binding activity of STAT3 (Ray et al. 2010).

ERp57 is known to be over-expressed in a variety of stress conditions (Lee 2001) and as shown from the results described above, this protein is also associated with MSH6, TMEM126A and Ets-1 gene sequences

Furthermore, our results obtained from *in vitro* binding assay with biotinylated DNA fragments corresponding to the gene of interest incubated

with M14 nuclear extract, have confirmed their association with ERp57 and their interaction with APE/Ref-1. Based on these data it is legitimate to speculate on the possibility that ERp57 binding MSH6 or TMEM126A or Ets-1, recruits APE/Ref-1 for protein complex formation in different cellular functions. Moreover, Ku86 and PARP-1 both protein involved in DNA repair are not able to bind MSH6, TMEM126A and Ets-1 biotinylated DNA fragments.

In conclusion, in M14 cells a potential MSH6 and TMEM126A regulatory sequence has been revealed to be a target of ERp57 and of APE/Ref-1. When ERp57 is knocked-down, both MSH6 and TMEM126A genes are down-regulated suggesting a regulation by ERp57 at transcriptional level.

7 Aim of the work II

Extensive oxidative stress is a common feature of neurodegenerative diseases, such as Amyotrophic Lateral Sclerosis, Alzheimer's disease and Parkinson's disease (PD). Oxidative stress is particularly important at the Endoplasmic Reticulum (ER) level, where proteins reach their native conformation with the help of a number of enzymes involved in the redox control of cysteine residues. If the ER luminal redox system is overwhelmed, the loss of the thiol-disulfide redox buffer can impair the oxidative protein folding causing luminal accumulation of unfolded/misfolded proteins which trigger the Unfolded Protein Respose (UPR). A role for redox imbalance and consequent ER dysfunction in neurodegenerative diseases has been suggested (Banhegyi et al. 2008), and recently the involvement in neurodegeneration of ERp57 has been pointed out (Erickson et al. 2005; Hetz et al. 2005; Kim-Han and O'Malley 2007). In particular, it has been demonstrated that in PD models, 6-hydroxydopamine (6-OHDA), a widely used parkinsonian mimetic, induces an alteration of ERp57 protein which undergoes post-translational modifications in rats striatum, suggesting an involvement of ER stress (Ogawa 2010). In addition, Kim-Han and O'Malley have demonstrated that 6-OHDA leads to the rapid formation of an ERp57-DNA aggresome in primary neuronal cells in culture (Kim-Han and O'Malley 2007).

The aim of the present work was to evaluate the modulation of the expression and cellular localization of ERp57 in neuronal cells in culture or *in vivo* in CD1 mice treated with a recently identified parkinsonian mimetic, 5-S-Cysteinyldopamine (CysDA).

We also studied the modulation of the expression, aggregation and cellular localization of α-Synuclein, which is a key protein in Parkinsonian neurodegeneration.

In recent years, CysDA has received great attention in view of its possible significance as an index of oxidative stress in aging and in neurodegenerative processes (Mosca et al. 2006). CysDA is a catecholthioether derivative arising from the nucleophilic addition of a thiol to the benzene ring of dopamine (DA) following its oxidation to an *o*-quinone (Zhang and Dryhurst 1994). DA-quinone addition to Glutathione (GSH), the most abundant thiol compound in the cell, gives rise to 5-S-glutathionyldopamine (GSH-DA) which is hydrolyzed by peptidases to form free CysDA.

GSH-DA levels in the brain are very low, and near the limit of detection, whereas CysDA levels are easily detectable. This latter compound has been identified long ago in autoptic brains of various mammalian species, and was found to be highest in humans compared to other mammals, particularly in the striatum (Rosengren et al. 1985).

It is also present in the cerebrospinal fluid of PD patients (Cheng et al. 1996) and there are circulating antibodies against CysDA in individuals affected by PD (Salauze et al. 2005).

This substance is able to induce apoptotic death via caspases activation, mitochondrial membrane depolarization and Complex I inhibition (Spencer et al. 2002; Mosca et al. 2006; Mosca et al. 2008).

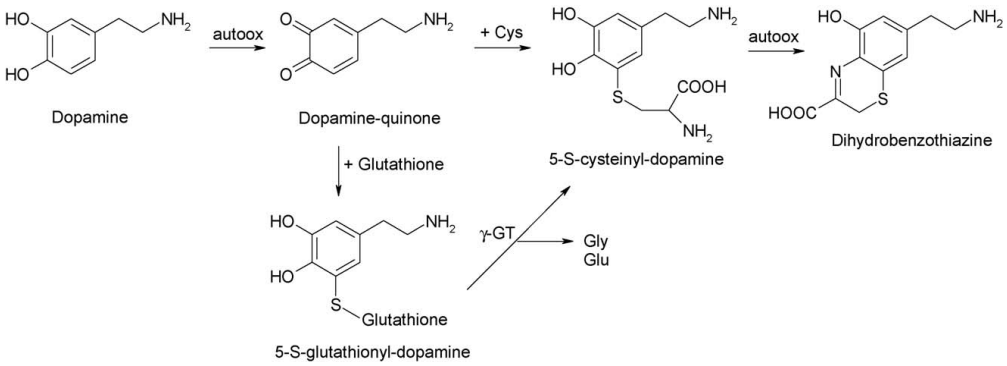

Figure 9. Proposed pathway of 5-S-cysteinyl-dopamine (CysDA) synthesis *in vivo*. Autooxidation of DA produces the highly reactive DA-quinone, that can undergo nucleophilic addition of thiol groups (both free cysteine or glutathione), giving rise mainly to the 5-S-isomer (the 2-S-Cys-DA and 2,5-S,S-di-Cys-DA isomers represent less than 20% of the total products *in vitro*). 5-S-glutathionyl-DA can then be converted to Cys-DA by peptidases, mainly g-GT. Cys-DA may be further oxidized to dihydrobenzothiazine derivatives.(Mosca et al. 2006)

Cys-DA has also drawn further attention as a putative precursor of neuromelanin, the characteristic pigment occurring in the bodies of dopaminergic neurons of *Substantia Nigra pars compacta* (SNc) and arising from the auto-oxidation and polymerization of DA and CysDA (Carstam et al. 1991; Zecca et al. 2001). A dramatic reduction of neuromelanin in SN is the distinctive anatomopathological feature of PD, which parallels the selective degeneration of the dopaminergic neurons of SN, along with the accumulation of intraneuronal cytoplasmic inclusions characterized by ubiquitinilated alpha-synuclein (α-Syn) aggregates, known as Lewy bodies (Venda et al. 2010).

α-Syn is a presynaptic protein which is natively unfolded, i.e. it can assume various conformations depending on the environmental conditions. The physiological role of α-Syn is to modulate DA function and metabolism

by interacting with key proteins involved in its metabolism and storage (Perez and Hastings 2004). A diverse array of evidence is emerging that α-Syn may undergo aggregation and fibril formation, leading to a loss of function, which in dopaminergic neurons may determine a dysregulation of the DA pathways with subsequent excess of cytosolic DA, that can enhance the neurotoxic effect of α-Syn aggregates (Perez and Hastings 2004). DA release into the cytosol can also trigger oxidative stress which might be responsible for the dysfunction and death of neuronal cells that contribute to pathogenesis and to further protein aggregation.

8 Materials and Methods II

8.1 Synthesis of CysDA

CysDA was synthesized as described by Chioccara and Novellino for CysDOPA (Chioccara and Novellino 1986). 20 mmol ceric ammonium nitrate in 100 ml of 2 M H_2SO_4 was added to a 10 mmol of DA in 2 M H_2SO_4. The resulting orange reaction mixture was immediately poured at once to a vigorously stirred solution of L-cysteine (5 g) in 50 ml of 2M H_2SO_4. The resulting blue solution was directly passed through a column (2 x 40 cm) of Dowex 50Wx8 (H+ form) equilibrated with water. After washing with water, the column was eluted with 0.5 N HCl to eliminate unreacted DA. Further elution with 3 N HCl and then 4 N HCl gave a mixture of various CysDA isomers (2-S- and 5-S-cysteinyldopamine, and 2,5-S,S-dicysteinyldopamine). The eluted fractions were combined, reduced to a small volume (2 ml) redissolved in water and rechromatographed on a Dowex 50Wx2 (2 x 40 cm) equilibrated with 2 N HCl. Elution was carried out with 2 N HCl and 10 ml fractions were collected and analyzed spectrophotometrically. The second peak eluted (fractions 50-100, with λmax 254 and 293 nm, relative absorbance 4:3) was collected and after removal of the solvent by freeze-drying gave CysDA as a pale brown residue. The purity of the product was checked by HPLC, which revealed no contamination by other isomers or unreacted dopamine and the identity of the substance was further confirmed by Electrospray Ion Mass Spectrometry (molecular mass: 272,1 Da). The concentration of CysDA in solution was checked

spectrophotometrically by using a molar extinction coefficient of 2860 $M^{-1}cm^{-1}$ at 293 nm.

8.2 Cell culture and treatment

The human dopaminergic neuroblastoma cell line SH-SY5Y was obtained by ICLC (Genova, Italy). The SH-SY5Y cell line has become a popular cell model for PD research because this cell line posses many characteristics of DAergic neurons. For example, these cells express tyrosine hydroxylase and dopamine-β-hydroxylase as well as the dopamine transporter (Xie et al. 2010). The cells were maintained in a humidified incubator under 5% CO_2 at 37°C, and were grown in Dulbecco's modified Eagle's/F12 medium supplemented with 10% heat-inactivated fetal bovine serum and 2 mM glutamine. The cells were routinely harvested twice a week by trypsinization (0.05% trypsin-EDTA) and plated in 25 cm^2 culture flasks (split 1:4-1:8). Cells at 50-60% confluence were treated with CysDA or 6-OHDA at a final concentration of 100 μM in culture medium and harvested at the indicated times. Cell viability was assessed by trypan blue exclusion.

8.3 Animals

Male CD1 mice (25-30 g of weight; Harlan Italy) were used. Upon arrival at the laboratory, the animals were housed in an air-conditioned room (temperature 21±1 °C, relative humidity 60±10%) with lights on from 8 to 20h. Males were housed in same-sex groups of 3 individuals in 32 x 14 x 12

x cm Plexiglas boxes with a metal top and sawdust as bedding, and with pellet food (standard diet purchased from Harlan Italy) and tap water *ad libitum*. Experimental subjects were weighed after the lesion. All the experiments were performed in strict compliance with the Italian National Laws (DL 116/92), the European Communities Council Directives (86/609/EEC). All efforts were made to minimize the number of animals used in the study and their suffering.

8.4 Surgical procedures

DA-denervating lesions were performed by bilateral injection of 6-OHDA or CysDA into the dorsal striatum as previously reported (Branchi et al. 2008).

Briefly, on the day of the surgery, mice received an intraperitoneal (i.p.) injection of the noradrenaline transporter inhibitor, desipramine (25 mg/kg, 30 min before surgery) and were anesthetized with equithesin (3 ml/kg, i.p.) [Na pentobarbital (0.972 g), chloral hydrate (4.251 g), magnesium sulfate (2.125 g), ethanol (12.5 ml), and propylene glycol (42.6 ml) in distilled water (total volume, 100 ml)] and positioned on a stereotaxic frame (Kopf Instruments, Tujunga, CA).

6-OHDA and CysDA (2 μg/μl) were separately dissolved in 0.2% ascorbate saline. Three different groups of animals were injected with 4 μl of 6-OHDA solution, CysDA solution, or a corresponding volume of saline (SHAM-operated mice) into the dorsal striatum at a flow rate of 0.5 μl/min using a 10 μl Hamilton microsyringe with a 30-gauge needle at the following coordinates: AP = + 1; ML = ± 1.7; DV = -2.9 mm, tooth bar −2.4 (relative to

bregma and midline, in mm). The needle was left in place for 5 min after the injection before retraction. Each animal received a total of 16 μg of 6-OHDA or CysDA, 8 μg at each side. After surgery, the animals were left undisturbed in their home cage for 21 days and their body-weight was daily monitored.

A fourth group of intact mice was housed as the 6-OHDA-, CysDA- and SHAM-operated rats, but left undisturbed in their home cage.

8.5 Monoamine and monoamine metabolites determinations

Mice were sacrificed at 21 days after lesion for the determination of DA, noradrenaline (NA), 5-hydroxytryptamine (5-HT) and their metabolites. For monoamine and monoamine metabolites assay, the brain was rapidly removed and the striata were dissected out on ice, weighed in polypropylene vials and homogenated in percloric acid (PCA) 0.1M. Samples were centrifuged for 20 min at 15000g (4°C), then the supernatant was used for monoamine and monoamine metabolites assays. The endogenous levels of DA, DA metabolites (homovanillic acid, HVA and 3, 4-dihydroxyphenylacetic acid, DOPAC), NA, 5-HT and 5-HT metabolite (5-hydroxyindolacetic acid, 5-HIAA) were assayed by microbore HPLC using a SphereClone 150-mm x 2-mm column (3-μm packing). The detection was accomplished with a Unijet cell (BAS) with a 6-mm-diameter glassy carbon electrode at +650 mV versus an Ag/AgCl reference electrode, connected to an electrochemical amperometric detector (INTRO, Antec Leyden, Netherlands). The chromatographic conditions were: (i) a mobile phase composed of 85 mM of sodium acetate, 0.34 mM EDTA, 15 mM sodium chloride, 0.81 mM of octanesulphonic acid sodium salt, 5% methanol (v/v),

pH = 4.85 (ii) a rate flow of 220 µl/min (iii) a total runtime of 65 min. For each analysis, a set of standards containing various concentrations of each compound (monoamines and their metabolites) was prepared in the acid solution. The calibration curves were calculated by a linear regression. The retention times of standards were used to identify peaks and peak area were used to quantify monoamine levels. Results were normalized to the weight of the wet tissue.

8.6 Detection of protein carbonylation by OxyBlot

The carbonyl assay is widely used to study oxidative protein damage in tissues and in cells. The reactive oxygen species (ROS) attack on aminoacid residues (namely His Arg Lys and Pro) generates carbonyls that can be detected after reaction with 2,4-dinitrophenylhydrazine. Brain specimens or treated cells were homogenized in 0.25 M sucrose, 100 µM TRIS-HCl buffer (pH 7.4) containing 100µM $MgCl_2$, 80 µM EDTA, and protease inhibitors, sonicated for 5 sec and centrifuged at 400g to remove debris, whereas cells were treated as above described to isolate nuclear and cytosolic proteins. Protein oxidation was measured by OxyBlot Protein Oxidation Detection Kit (Millipore), following manufacturer instructions. Briefly, samples (5 µl) were derivatized at room temperature for 20 min in 10

mM 2,4-dinitrophenylhydrazine (DNPH) and 5 µl of 12% sodium dodecyl sulfate (SDS). Samples were neutralized with 7.5 µl of neutralization solution (2 M Tris in 30% glycerol). Derivatized samples (250 ng) were then blotted onto a nitrocellulose membrane under vacuum using a slot-blot apparatus (Bio-Rad). Membranes were blocked with 3% BSA in Tris Buffer saline containing 0.1% Tween (TBS-T) for 1h and next incubated with rabbit antibody to protein-bound DNP (diluted 1:150) for 90 min. After washing with TBS-T, membranes were incubated with anti-rabbit IgG alkaline phosphatase secondary antibody (1:5000) in TBS-T for 1 h at room temperature. The membrane was washed in TBS-T and developed using a solution of nitrotetrazolium blue chloride (0.2 mM) and 5-bromo-4-chloro-3-indolyl phosphate dipotassium (0.4 mM) in alkaline phosphate buffer (0.1 M Tris, 0.1 M NaCl, 5 mM $MgCl_2$; pH 9.5). Dried blots were quantified using QuantityOne image analysis (BioRad).

8.7 Determination of GSH/GSSG

Glutathione (GSH) is one of the most important cellular antioxidants. It acts as a thiol buffer in the cells and is important in the detoxification of potentially harmful endogenous compounds and xenobiotics. GSH can be

readily oxidized to its disulfide (GSSG) and the ratio of both forms is crucial for the characterization of the oxidative stress in cells.

GSH and GSSG were determined by HPLC after their derivatization with OPA to form a stable, highly fluorescent tricyclic derivate (Hissin and Hilf 1976). Tissue specimens and treated cells were resuspended in cold 10% metaphosphoric acid. After incubation at 4°C for 15 min, the mixtures were centrifuged (20000g, 15 min, 4°C) and supernatants stored at −80°C until analysis by HPLC. To determine GSH, 50 µl of the supernatant were treated with 1.0 ml of 0.1% EDTA in 0.1M phosphate buffer, pH 8.0. 20 µl of this mixture were treated with 300 µl of 0.1% EDTA in 0.1M phosphate buffer, pH 8.0, as a diluent, and 20 µl of 0.1% OPA in methanol. After incubation at 25°C for 15 min in the dark, the mixture was filtered and analyzed by HPLC. To determine GSSG, 200 µl of the supernatant were incubated at 25°C with 200 µL of 40 mM N-ethylmaleimide (NEM) for 25 min in the dark, then 750 µl of 0.1 M NaOH were added. 20 µl of this mixture were used for HPLC analysis, using the procedure above described for GSH, except that 0.1 M NaOH was employed as diluent.

The HPLC system consisted of a Waters apparatus, equipped with a 600 pump and pump controller, a Waters 717 plus autosampler, an X-Bridge column (C18 reverse phase, 4.6x250mm, 5µm particle size - thermostated at

37°C with a 10mm guard column of the same material matrix) and a Shimadzu RF-551 spectrofluorometric detector.

The mobile phase consisted of 15% methanol in 25 mM phosphate buffer, pH 6.0. The flow rate was kept constant at 0.5 ml/min. The excitation/emission wavelengths were set at 350/420 nm.

Peak identification and quantitation was performed by automatic peak area integration using a dedicated software (Millennium32, Waters).

8.8 Western Blot analysis

Nuclear and cytosolic proteins were obtained from treated SH-SY5Y cells by ProteoJET™ Membrane Protein Extraction Kit (Fermentas, M-Medical srl, Milan, Italy). To verify the correct separation of the two fractions, a Western Blot was performed by using specific antibodies againt Lamin A and C (Millipore, Vimodrone, Milan, Italy) and Vinculin (Santa Cruz Biotechnology, Inc., DBA Italia, Segrate, Milan, Italy), specific for the nuclear and cytosolic fractions, respectively.

Brain tissues were treated with ice-cold lysis buffer (0.10 mM Tris pH 8, 0.25 M sucrose, 0.10 mM $MgCl_2$, 0.80 mM EDTA) containing 1 mM PMSF and 1% protease inhibitor cocktail (Roche) and immediately

homogenized with 15 pestel strokes using a Dounce glass homogenizer. The homogenate was sonicated for 5 sec on a LABSONIC M sonicator (B.Braun Biotech International) at an amplitude of 60, and centrifuged at 12000g for 5 min to remove debris.

Tissue lysates and cell extracts were separated by electrophoresis on SDS-PAGE on 12% Mini-PROTEAN® TGX™ Precast Gel (Biorad Laboratories) followed by transfer to a Protran® Nitrocellulose Membrane (Whatman GmbH, Dassel, Germany). The membrane was blocked with 5% non fat dry milk in PBS-T buffer for 1 h at room temperature prior to incubation overnight at 4°C with two different primary antibodies, i.e. anti-α-Syn (Cell Signaling, 1:500) or anti-ERp57 (1:300, polyclonal antibody obtained by immunizing rabbits with ERp57 purified from pig liver (Chichiarelli et al. 2007)).

The proteins were visualized by ECL detection kit (GE Healthcare).

8.9 Real time RT-PCR determination of ERp57 and α-Syn

To analyze the expression of ERp57 and α-Syn mRNA, total RNA was extracted from adherent cells using TRIZOL® reagent (Invitrogen Corporation, Carlsbad, CA, USA) in accordance with the manufacturer's

instructions. Briefly, 10^7 cells were washed with ice-cold PBS and lysed in 1ml of TRIZOL reagent. The RNA pellet was resuspended in diethyl pyrocarbonate (DEPC) treated water and stored at -80°C until use. An aliquot of each RNA was loaded onto 1% agarose gel to visualize and quantify the degree of RNA integrity. cDNA was synthesized from 1,5 μg of total RNA using as reverse trascriptase QuantiTect® Reverse Transcription Kit (Qiagen) in accordance with the manufacturer's instructions, and analyzed by real-time polymerase chain reaction (qPCR). cDNA concentration was determined using a GeneQuant II RNA/DNA Calculator (Pharmacia Biotech).

The Two-step SYBR-Green I-based real time RT-PCR was carried out using an MJ MiniOpticon™ Detection Systems (Bio-Rad Laboratories, Milan, Italy). Amplification was carried out with 500 ng of cDNA, using Maxima®SYBR green qPCR Master mix (2x) (Fermentas, Milan, Italy) in a final volume of 25 μl. Each sample was analyzed in triplicate. PCR conditions were 95°C for 10 minutes followed by 40 cycles of 95°C for 15 seconds and 60°C for 1 minute.

To amplify mRNA the following primers were used:

-ERp57 primers were purchased from Qiagene (ERp57 or PDIA3, Ref.Seq Accession: NM_005313.4).

-α-Syn primer was designed by MWG-Biotech AG using Primer Express software (Applied Biosystems) and were synthesized by Primm

(Milan, Italy):

forward primer: 5' CGA AGT CTT CCA TCA GCA GTG 3’

reverse primer: 5' AAG GGA AGC ACC GAA ATG 3'

The results were analyzed using the Gene Expression Macro™, Version 1.1 (Bio-Rad), which recorded the threshold cycle (Ct).

Untreated cell sample (CTL) was used as control and target gene Ct values were normalized against RPS27A (RPS27A_2_SG, Ref.Seq Accession: NM_002954, obtained from Qiagen). Data were analyzed using the $2^{-\Delta\Delta Ct}$ method and expressed as fold change compared with CTL (Relative Quantity).

8.10 Protein determination

Protein content of cellular and tissue homogenates was evaluated by the BioRad reagent (Bio-Rad Laboratories, Segrate, Milan, Italy) using bovine serum albumin as a standard.

8.11 Statistical analyses

Experiments were repeated at least three times and all the results are expressed as the mean value ± Standard Deviation (SD). Statistical comparison between groups was made using Student's t test or post hoc anova (Tukey's). p values<0.05 were regarded as significant.

9 Results II

9.1 CysDA induces selective DA depletion in the striatum

Among PD animal models, one of the most commonly used is the induction of neuronal lesion by the intrastriatal injection of 6-OHDA in rats or mice. This latter substance is one of the known parkinsonian mimetics and is widely used to study mechanisms of cell death of dopaminergic neurons in PD, providing permanent dopaminergic depletion selective to the nigrostriatal pathway by stereotaxic surgical administration (Blandini et al. 2008).

CysDA was found to be highly neurotoxic *in vitro*, both on primary neural cells and on immortalized neuroblastoma dopaminergic cells (Spencer et al. 2002; Mosca et al. 2006). In this study we aimed at verifying whether the intrastriatal injection of CysDA caused the same degenerative effects exerted by 6-OHDA. To this purpose, the effect of this substance on catecholaminergic neurotransmitter levels, the rate limiting enzyme in neurotransmitter synthesis, were evaluated in brains of mice subjected to DA-denervating lesions by bilateral injection of either CysDA or 6-OHDA.

Following both CysDA and 6-OHDA injections, DA concentration in the striatum was significantly reduced (Fig. 10A).

A)

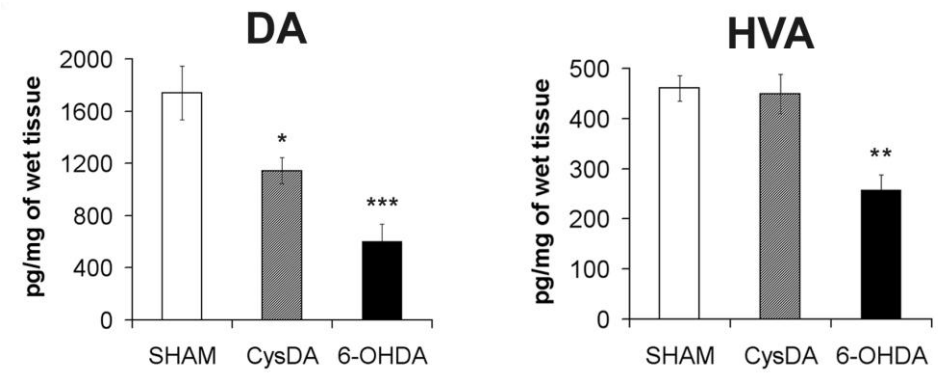

B)

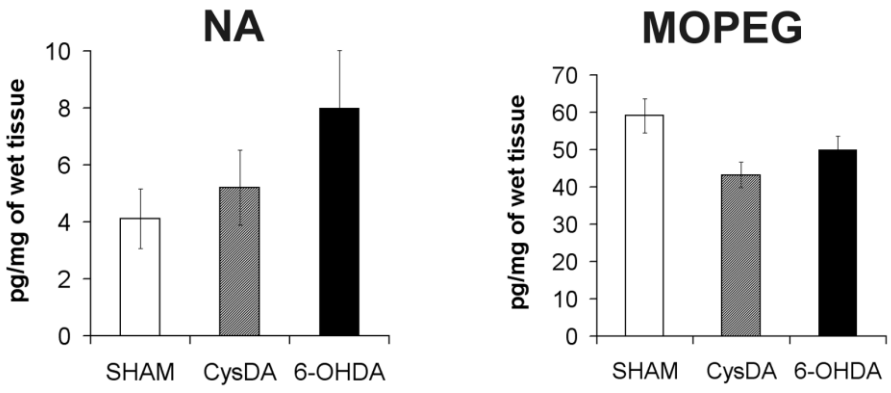

C)

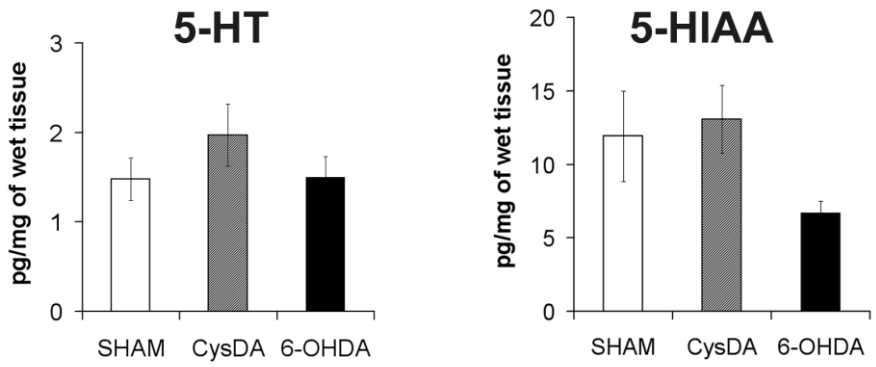

Figure 10. Neurotransmitter levels in the brains of mice treated with CysDA or 6-OHDA. Following both CysDA and 6-OHDA injections in the striatum, as described in Material and Methods, the neurotransmitter levels were determined by HPLC analysis. **A)** Dopamine (DA) and its metabolite homovanilic acid (HVA) as a sign of neurological damage; **B)** noradrenaline (NA) and its metabolite 3-methoxy-4-hydroxyphenylethyleneglycol (MOPEG); and **C)** serotonin (5-HT) an its metabolite 5-hydroxyindoleacetic acid (5-HIAA). Values are expressed as pg of neurotransmitter/mg of wet tissue. Data represent the mean of at least three independent experiments ± S.D. *$p<0.05$ vs SHAM-operated mice; **$p<0.01$ vs SHAM-operated mice; ***$p<0.001$ vs SHAM-operated mice.

In particular, post hoc Tukey's test indicated that CysDA treatment induced a 35% reduction in DA concentration compared to SHAM-operated mice ($p<0.05$), whereas the lesion induced by 6-OHDA was more pronounced, leading to a 65% reduction in DA ($p<0.001$). The DA turnover (calculated as the HVA/DA ratio) was not affected by both neurotoxins (Fig.10A). Moreover, no significant effect on noradrenergic and serotonergic neurotransmission was evidenced in the striatum of mice injected with

CysDA or 6-OHDA (Fig. 10B and C). Likewise, NA turnover (calculated as the MOPEG/NA ratio) and 5-HT turnover (calculated as the 5-HIAA/5-HT ratio) were not affected.

9.2 CysDA treatment of both SH-SY5Y cells and mice brains induces extensive oxidative stress

It is ascertained that the toxic properties of CysDA and of 6-OHDA are mediated by their ability to induce oxidative stress, which has a prominent role in the neurodegenerative process of PD (Mosca et al. 2006; Miller et al. 2009; Reiter et al. 2010). Evidences suggest that dopaminergic neurons may be particularly vulnerable to oxidative injury, thus ROS generation due to the catecholamine metabolism could account, at least in part, for the selective degeneration of these neurons (Fahn and Cohen 1992; Dauer and Przedborski 2003). In particular, several reports indicate that the GSH-GSSG equilibrium is seriously compromised in parkinsonian brains (Sian et al. 1994) and that protein carbonylation increases with age and in neurodegenerative diseases (Alam et al. 1997; Sultana et al. 2009).

- *GSH/GSSG detection*

Glutathione plays important roles in biological systems, primarily in the detoxification of potentially harmful xenobiotics and in the antioxidant defence response. It can be readily oxidized to its disulfide and the ratio of both forms is crucial for the characterization of the oxidative stress in cells. Indeed oxidative stress in neurodegeneration has a profound effect on the cellular thiol balance and can lead to a decreased GSH/GSSG ratio and to a decrease of the total amount of GSH (Sofic et al. 1992; Sian et al. 1994).

GSH and GSSG amounts were determined in different brain regions of mice treated with CysDA or 6-OHDA. The analysis revealed that the levels of GSH and GSSG were comparable in striatum, hippocampus and prefrontal cortex of SHAM-operated mice (Fig. 11A). In these animals GSH amount was found to be about 1 μmol per gram of tissue, whereas GSSG was about 0.25 μmol per gram of tissue. Compared to SHAM-operated mice, CysDA- and 6-OHDA-treated mice showed significantly reduced levels of GSH in all brain areas. Conversely, the amount of GSSG does not seem to be affected by both neurotoxins treatment in any brain area.

A)

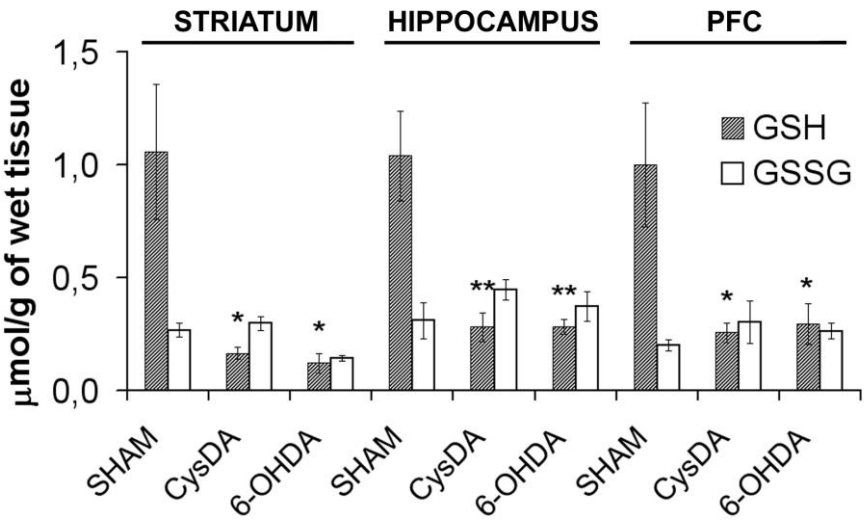
STRIATUM
HIPPOCAMPUS
PFC
µmol/g of wet tissue
1,5
1,0
0,5
0,0
GSH
GSSG
SHAM
CysDA
6-OHDA
SHAM
CysDA
6-OHDA
SHAM
CysDA
6-OHDA

B)

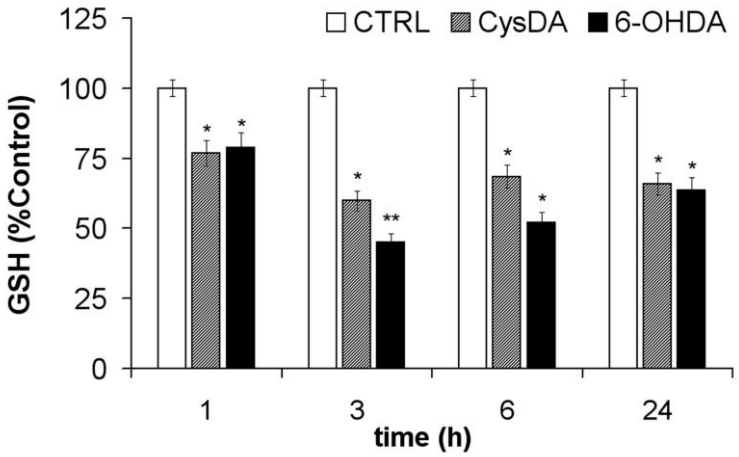
CTRL
CysDA
6-OHDA
GSH (%Control)
125
100
75
50
25
0
1
3
6
24
time (h)

C)

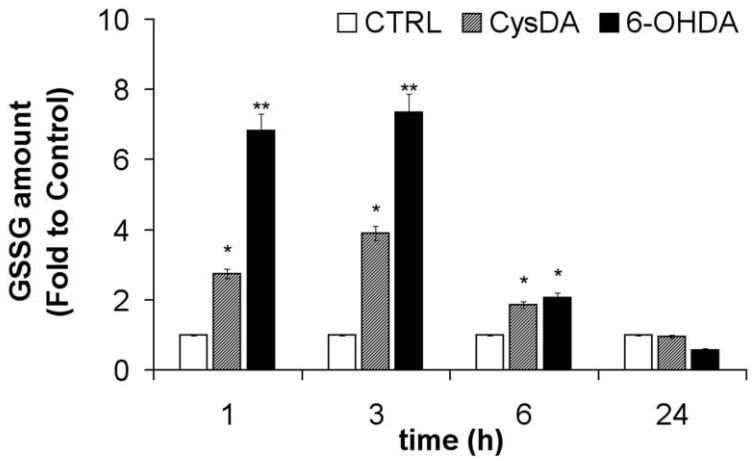

Figure 11. GSH levels in brains and in cells after CysDA and 6-OHDA treatment. GSH and GSSG were determined by HPLC with fluorometric detection after derivatization with OPA as described in Materials and Methods. **A)** GSH and GSSG levels in different brain areas of SHAM-operated mice or mice treated with CysDA or 6-OHDA. Data are expressed as μmol/g of tissue (fresh weight). Data represent the mean of n=6 different brain specimens ± S.D. *p<0.05 and **p<0.01 versus SHAM-operated mice.
B) GSH amount (% versus control) in cells treated with 100 μM CysDA or 6-OHDA at various times. **C)** GSSG increase (fold to control) in cells treated with 100 μM CysDA or 6-OHDA at various times. Data represent the mean of at least three independent experiments ± S.D. *p<0.05 and **p<0.01 versus control cells (CTRL).

The kinetics of GSH oxidation was evaluated in SH-SY5Y cells exposed to CysDA or 6-OHDA at various times. The data revealed that GSH rapidly reacted to oxidative stress induced by both neurotoxins. Evaluation of the net amount of GSH in CysDA or 6-OHDA treated cells, indicated a rapid depletion of GSH by about 40 or 55%, respectively, within 3 hours, which

was persistent up to 24 hours (Fig. 11B). Within 1 hour of treatment, the amount of GSSG was more than six times higher in 6-OHDA-treated cells and 3 times higher in CysDA-treated cells compared to controls, reaching a seven-fold increase and four-fold increase, respectively, after 3 hours of treatment (Fig. 11C). The amount of GSSG returned to basal level in prolonged incubations, up to 24 hours.

- *Protein carbonylation*

Oxidative stress may also induce protein damage, which can be evaluated by assessing the level of protein carbonylation in brain. Reactive oxygen species (ROS) are able to react with amino acid residues thus producing carbonyl groups which can be measured spectrophotometrically after reaction with 2,4-dinitrophenylhydrazine. To evaluate whether CysDA and 6-OHDA treatment in mice induced protein carbonylation, different brain regions were isolated and analyzed. A significant increase in protein carbonylation was detected in the striatum which is the prime target of the neurotoxins (Fig. 12A).

A)

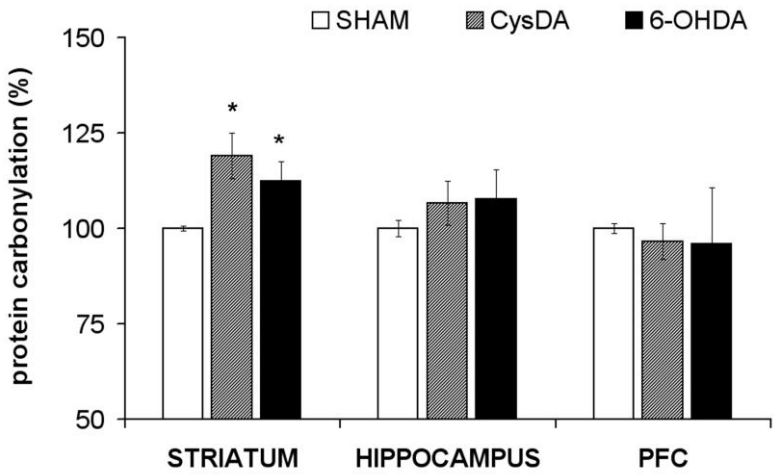

B)

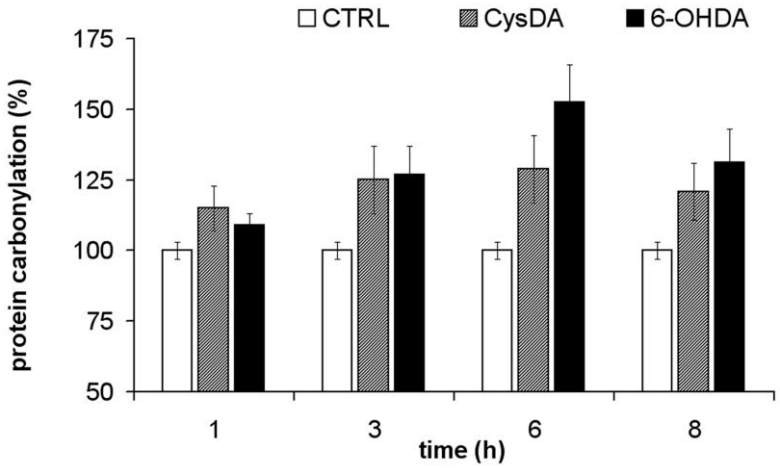

Figure 12. Protein carbonylation levels in brains and in cells after CysDA and 6-OHDA treatment. Proteins obtained from **A)** different regions of mice brains or from **B)** SH-SY5Y cells treated with 100 μM CysDA or 6-OHDA at various times, were analyzed by OxyBlot as described in Materials and Methods. Briefly, cells lysates or brain homogenates were derivatized with DNPH, blotted onto nitrocellulose membranes and probed with anti-DNP protein adducts polyclonal antibody. Data represent the mean of at least three independent experiments or n=6 brains specimens ± S.D. *$p<0.05$ respect to SHAM-operated mice or control cells (CTRL).

In this brain region, both CysDA and 6-OHDA induced a significant increase in protein carbonyls by about 20% compared to controls, whereas in the hippocampus a 10% increase in carbonyls can be observed. At the prefrontal cortex level, protein carbonylation seems not to be affected by both neurotoxins.

The time course of protein carbonylation was studied in the cellular model of PD, in which SH-SY5Y cells were treated either with CysDA or with 6-OHDA. When cells were exposed to the neurotoxins, a relevant increase in protein carbonylation was observed, reaching a maximum after 6h of incubation at 24 h (Fig. 12B).

9.3 CysDA modulates ERp57 levels and α-Syn aggregation

It is well known that oxidative stress induces a cellular response which involves the endoplasmic reticulum and a number of proteins whose expression and aggregation are influenced by the redox status of the cell. In particular we have analyzed protein levels in various brain regions and cellular fractions by Western blot, focusing our attention on ERp57, the stress protein which has been recently linked to neurodegeneration and on α-Syn, a key protein in Parkinson disease.

As regards Erp57, the level of this protein was found to be increased in the striatum, whereas in the hippocampus and at the cortex level no effect can be evidenced (Fig. 13A and B).

A)

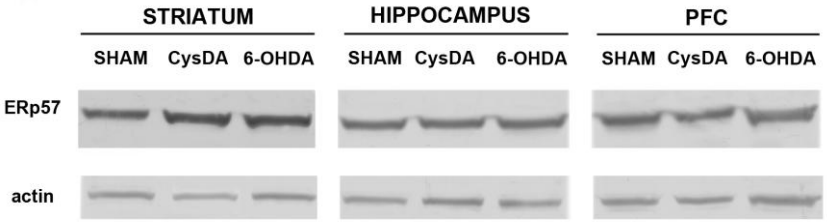

B)

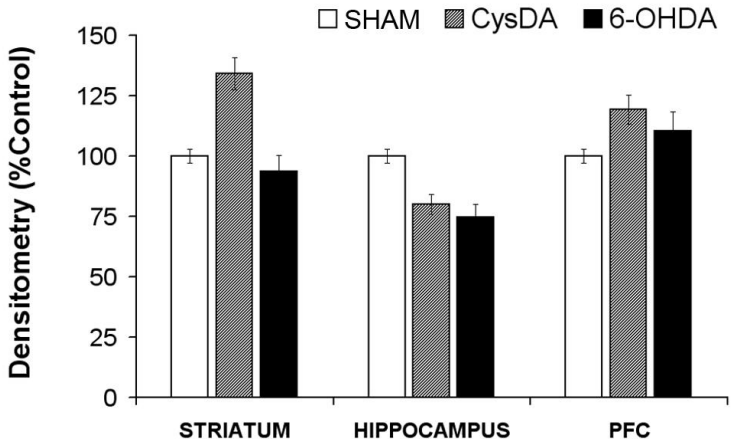

Figure 13. Western blot with ERp57 antibodies in mice brains.
A) Representative Western blot obtained from different brain regions. Proteins (≈70 µg) were loaded onto 12% SDS-PAGE gel, blotted onto nitrocellulose membrane and incubated with specific antibodies against ERp57. The bands were revealed by ECL chemiluminescence kit. **B)** Densitometric analyses of bands corresponding to ERp57 protein after CysDA or 6-OHDA treatment were performed with ImageJ software, and normalized to β-actin. Data are reported as percentage of control values, i.e. SHAM-operated mice, and are the mean ± S.D. of at least three brain specimens.

.ERp57 level in cells treated with both neurotoxins, was increased up to 24 hours at the cytosolic level on the contrary ERp57 was transiently increased within 3 hours in the nuclei (Fig. 14A and B).

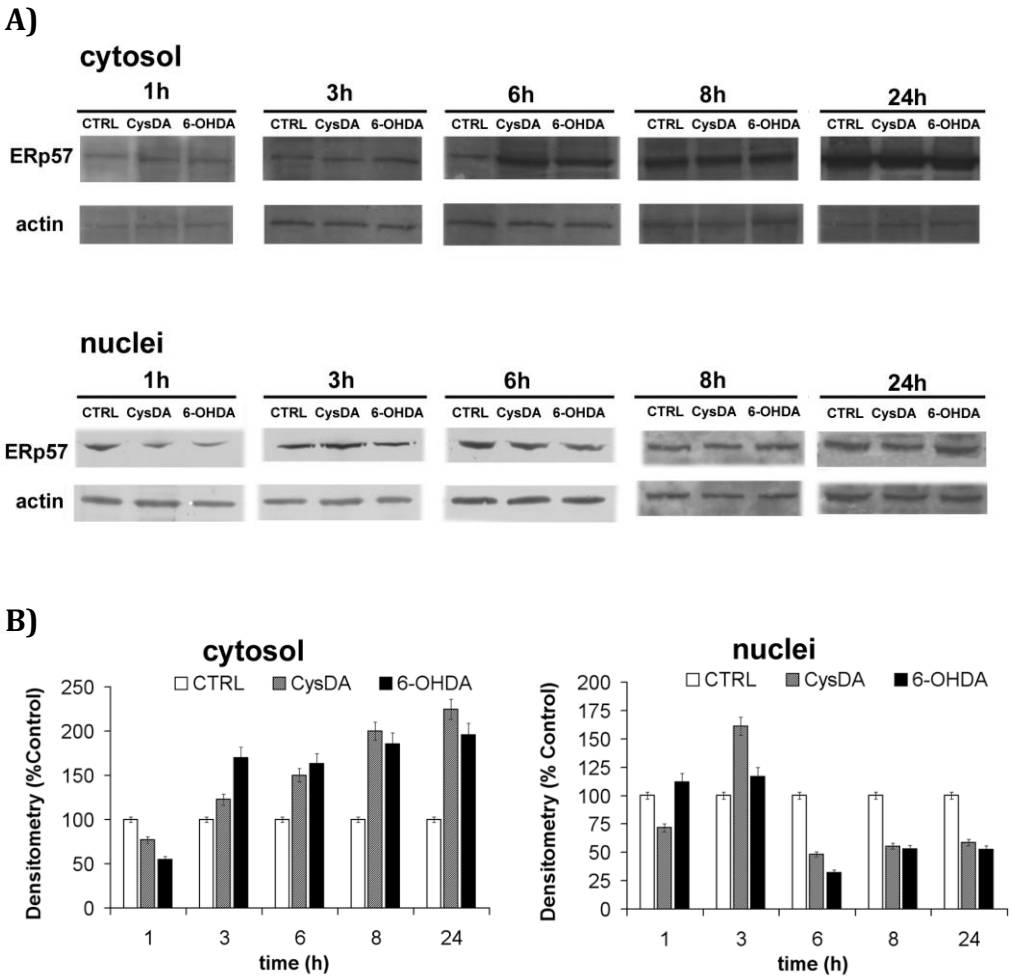

Figure 14. Western blot with ERp57 antibodies in SH-SY5Y cells.
A) Representative Western blot of ERp57 protein of cytosol and nuclei obtained from SH-SY5Y cells treated with 100 μM CysDA or 6-OHDA at various times. Proteins (≈70 μg) were loaded onto 12% SDS-PAGE gel, blotted onto nitrocellulose membrane and incubated with specific antibodies against ERp57. The bands were revealed by ECL chemiluminescence kit. Cytosolic and nuclear fractionation was verified by using Vinculin and Lamin A and C specific antibodies. **B)** Densitometric values of cytosol and nuclei were quantified by using ImageJ software and normalized to Vinculin and Lamin A and C. Each value represents the mean ± SD of at least three independent experiments and is given as percentage of control cells (CTRL).

Western blot analysis allowed to detect both the monomeric α-Syn form, which has an apparent molecular weight (MW) of 18kDa, and the dimeric form at 36 kDa. The presence of oligomeric forms could also be evidenced, with MWs higher than 54 kDa. For quantification purposes, only the momeric and dimeric forms were analyzed, due to the extreme variability and heterogeneity of the oligomeric forms. After mice treatment with CysDA and 6-OHDA, a two-fold increase in dimeric α-Syn form was observed specifically at the prefrontal cortex level with respect to SHAM-operated mice. On the contrary, the monomeric form seemed not to be affected in any cerebral area (see Fig.15 A and B).

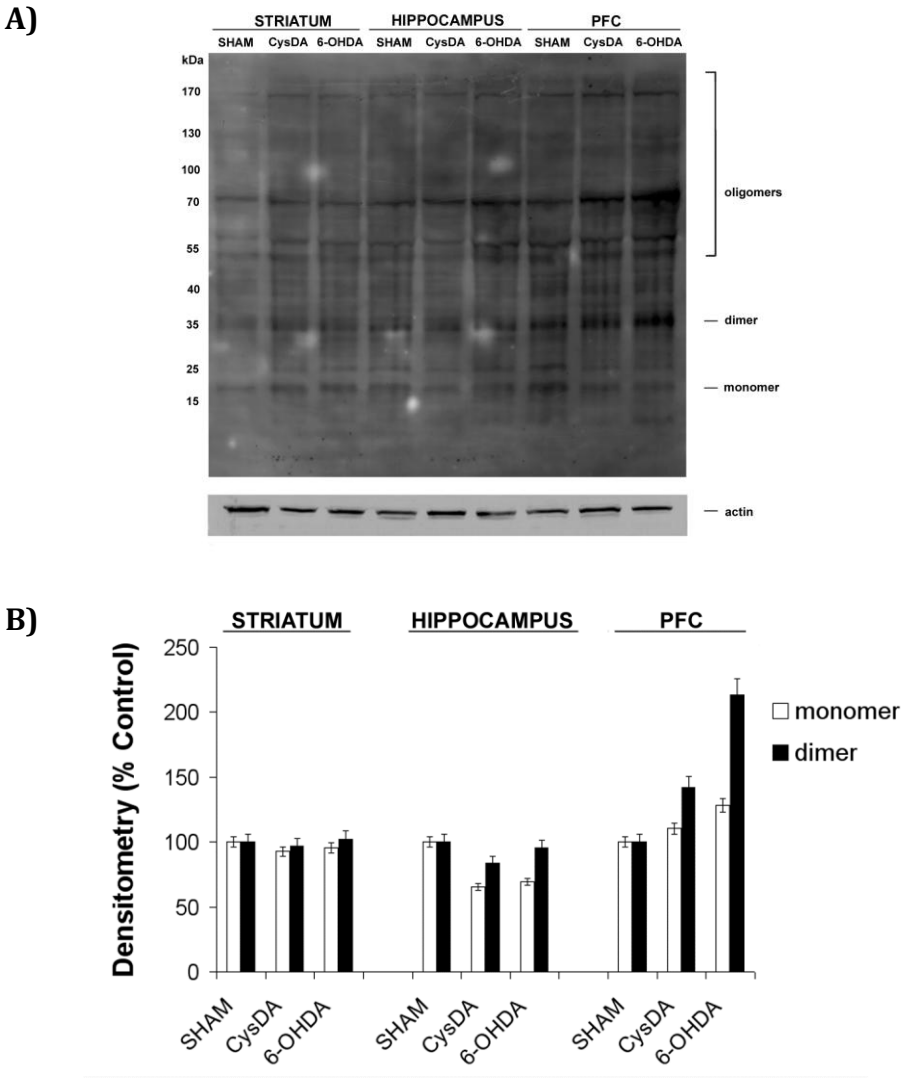

Figure 15. Western blot with α-Syn antibodies in mice brains.
A) Representative Western blot obtained from different mice brain regions treated with CysDA or 6-OHDA. Proteins (≈70 µg) were loaded onto 12% SDS-PAGE gel, blotted onto nitrocellulose membrane and incubated with specific antibodies against α-Syn. The bands were revealed by ECL chemiluminescence method. **B)** Densitometric analyses of bands corresponding to the monomeric (≈18kDa) and to the dimeric (≈36kDa) forms of α-Syn after CysDA or 6-OHDA treatment were performed with ImageJ software, and normalized to β-actin. Data are reported as percentage of control values, i.e. SHAM-operated mice, and are the mean ± S.D. of at least three brain specimens.

To assess α-Syn level and cellular localization, cytoplasm and nuclei fractions were obtained from SH-SY5Y cells treated with CysDA and 6-OHDA at various times. In the cytosol, both neurotoxins treatment induced a time-dependent increase in dimeric α-Syn level, whereas the monomeric form was increased within 1h and decreased in prolonged incubations, being absent at 24 hours (Fig. 16A and B). In the nuclei, only the monomeric form was present and was decreased compared to control within 8 hours of treatment, while at 24 hours it was found to be absent like in the cytosolic compartment (Fig. 16A and B).

A)

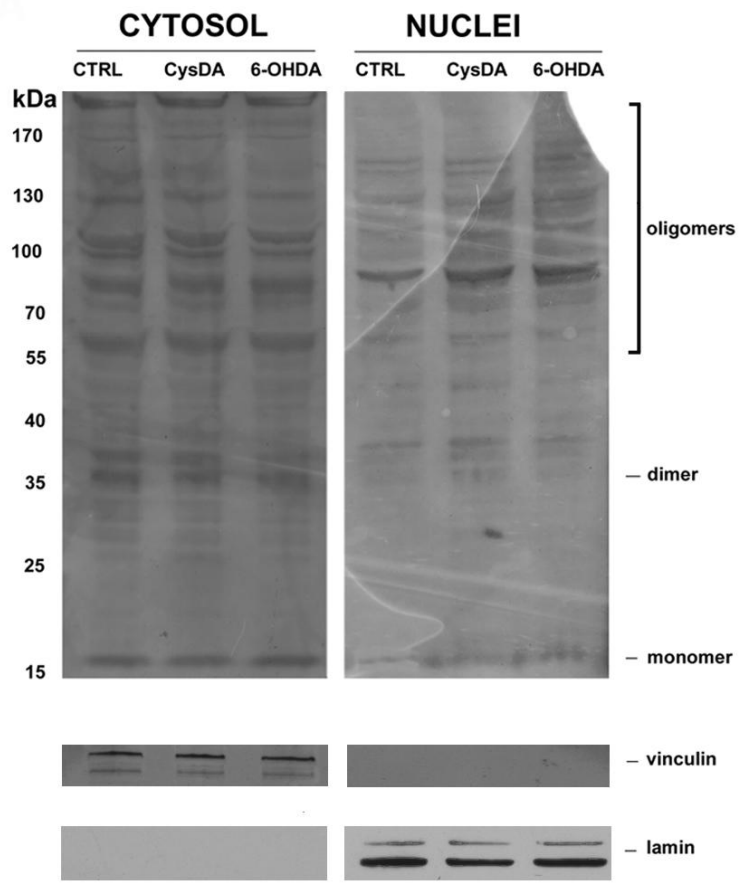

B)

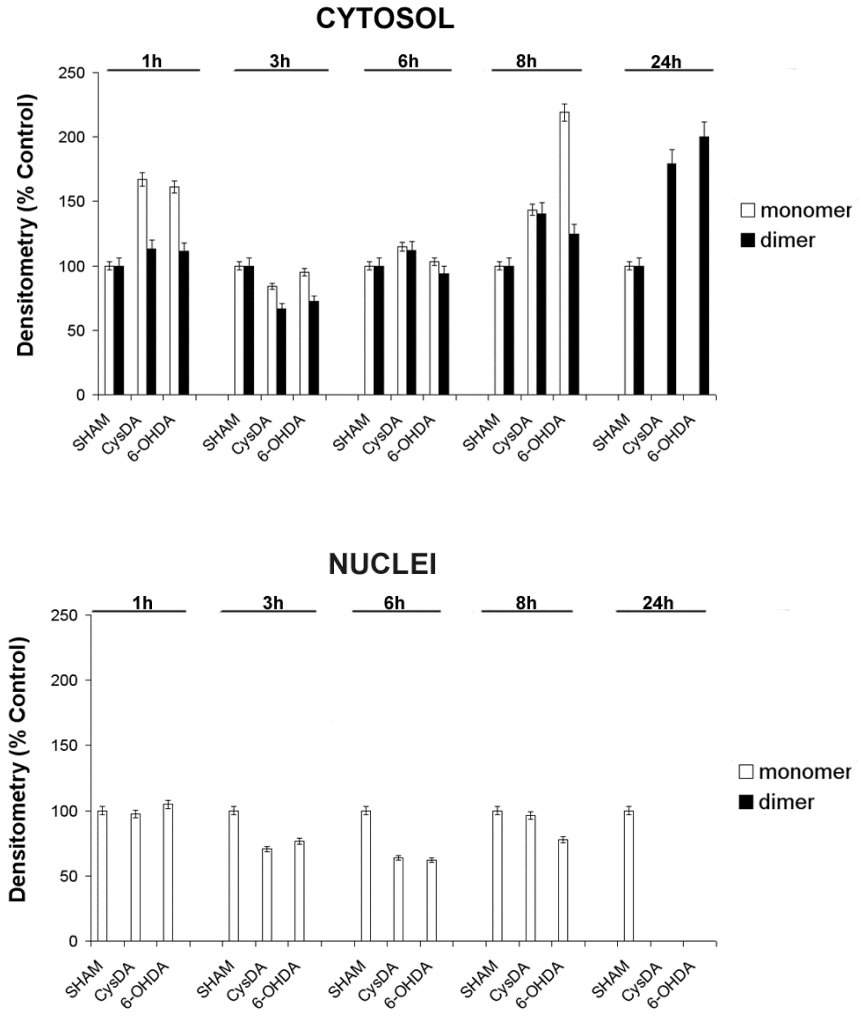

Figure 16. Western blot with α-Syn antibodies in SH-SY5Y cells. A) Representative Western blot obtained from cytosol and nuclei fractions of SH-SY5Y cells treated with 100 μM CysDA or 6-OHDA for 3 hours. Proteins (≈70 μg) were loaded onto 12% SDS-PAGE gel, blotted onto nitrocellulose membrane and incubated with specific antibodies against α-Syn. The bands were revealed by ECL chemiluminescence method. Cytosolic and nuclear fractionation was verified by using Vinculin and Lamin A and C specific antibodies. **B)** Densitometric values of α-Syn bands present in the cytosol or nuclei after CysDA or 6-OHDA treatment. Optical density was quantified by using ImageJ software, and normalized to Vinculin or Lamin A and C, respectively. Each value represents the mean ± SD of at least three independent experiments and is given as percentage of control cells (CTRL).

9.4 CysDA induces an increase of ERp57 and α-Syn gene expression

Because several neurotoxin such as MPP^+ and isoquinoline derivatives induced α-Syn increase, the expression level of ERp57 and of α-Syn mRNA from SH-SY5Y cells exposed to CysDA or to 6-OHDA were evaluated.

The real time amplification of the specific primers relatives to ERp57 and α-Syn genes was compared to RPS27A gene, used as endogenous control. ERp57 expression was increased within 3 hours and returned to basal level within the 24 hours of incubation (Fig. 17A). 6-OHDA treatment gives rise to the same expression trend for the two genes, but with a lower mRNA level compared to CysDA treatment.

The quantification of the relative transcript levels, from three independent experiments, demonstrated that after CysDA treatment, α-Syn expression was significantly upregulated within 6 hours up to four-fold compared to controls (Fig. 17B)

A)

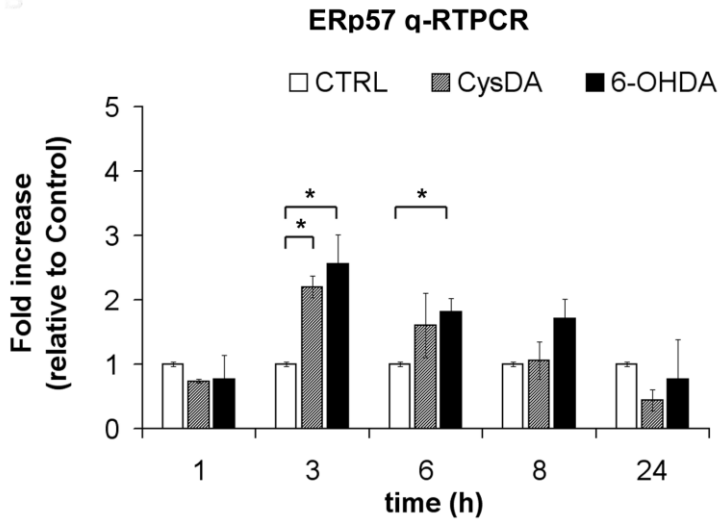

B)

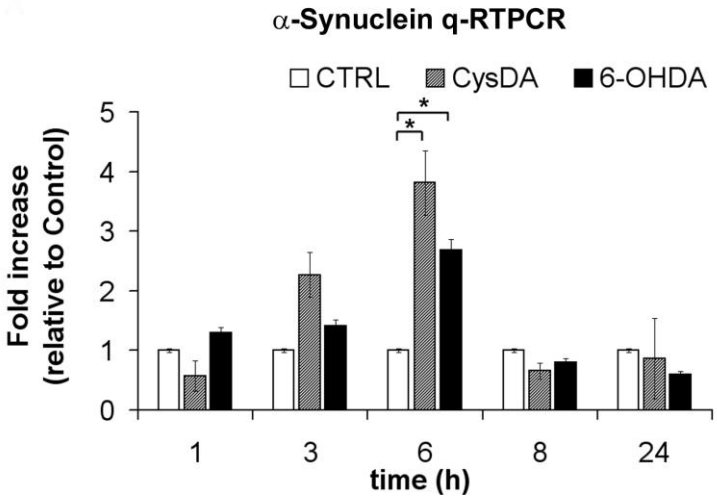

Figure 17. qRT-PCR of ERp57 and α-Syn.
mRNA was extracted from SH-SY5Y cell treated or untreated with CysDA and 6-OHDA, as described in Material and Methods. RPS27A (QuantiTect® QIAGEN) gene was used as reference for normalization and fold inductions were calculated using the formula $2^{-(\Delta\Delta Ct)}$. The relative quantification was analyzed using Gene Expression analysis for iCycler iQ real-time PCR detection system software, Version 1.10 (Bio-Rad Laboratories, Ltd.). The values represent the mean ± SD of at least three independent experiments. * $p < 0.05$ versus control cells (CTRL)..

10 Discussion II

Although the pathological phenotype and clinical symptoms of PD are well described, its aetiology and the mechanism(s) responsible for the neurodegeneration are still poorly understood. Genetic forms of the disease account for only 5-10% of cases of PD, while the rest are sporadic forms of unknown origin, hence a combination of environmental factors and genetic susceptibility has been proposed to justify the onset of the disease in most cases (Olanow and Tatton 1999).

The finding that the meperidine analog MPP^+ is able to induce selective neurodegeneration of catecholaminergic neurons in humans thus causing clinical manifestations typical of PD, has prompted research for endogenous substances which may be responsible for selective dopaminergic neurodegeneration in PD. Recent evidence point to CysDA as an endogenous neurotoxin. CysDA is a catecholthioether which, along with DA, is the building block of neuromelanin, the characteristic pigment of SN. Neuromelanin synthesis is an important protective process because the melanic pigment is thought to be responsible of the removal of reactive/toxic species that would otherwise cause neurotoxicity (Zucca et al. 2004). However, if the neuromelanin pathway is impaired, deleterious DA-quinone

species accumulation such as o-semiquinones can sequester GSH and then generate excess catecholthioethers and in turn benzothiazines. These compounds are potent inhibitors of mitochondrial pyruvate dehydrogenase (i.e., complex I/Krebs cycle) and complex I of the respiratory chain, and can promote α-synuclein fibrillization (Mazzio et al. 2011).

Neurotoxins which are known to be responsible for neurodegeneration in PD (i.e. 6-OHDA, MPP^+, paraquat, rotenone) have some common features: they are able to induce oxidative stress, to inhibit complex I of the respiratory chain and to be selectively toxic to dopaminergic cells. Most of these characteristics have been proven to be also typical of CysDA (Spencer et al. 2002; Mosca et al. 2006; Mosca et al. 2008). Furthermore, CysDA was demonstrated to disrupt DA trafficking *in vivo* and *in vitro*, thus interfering with DA uptake and possibly contributing to striatal neurodegeneration in PD (Sidell et al. 2001).

The first aim of the present study was to demonstrate whether CysDA could exert neurotoxicity *in vivo*. The data obtained demonstrate that intrastriatal injection of CysDA in CD1 mice caused a depletion of DA, without affecting serotonergic or noradrenergic systems. CysDA effect was similar to that observed for 6-OHDA, though the DA deficit was less pronounced. This effect may reflect an intrinsic difference between the two drugs, i.e. 6-OHDA probably leads to a more rapid and thus less chronically

progressive lesion of the nigro-striatal pathway compared to CysDA. The less pronounced toxicity of CysDA that we observed could actually represent an advantage in animal models of PD, given the chronic and long-lasting nature of the disease. This data suggest that CysDA may exert its selective neurotoxic effect by entering the cells through the dopamine transporter as already demonstrated for MPP^+ (Storch et al. 2004).

10.1 CysDA can induce oxidative stress both *in vivo* and *in vitro*

Previous work has demonstrated that CysDA is able to induce an increase in Reactive Oxygen Species in neuronal cells in culture, along with caspases activation and induction of mitochondrial dysfunction (Spencer et al. 2002; Mosca et al. 2008). Data regarding the prooxidant effect of CysDA *in vivo* are lacking, hence we aimed at verifying whether CysDA may alter the level of the typical oxidative stress markers, such as protein carbonyls and GSH levels in mice brains and in cells.

Different authors detected protein carbonylation in the striatum of PD affected patients and in other brain regions such as the cerebellum and the prefrontal cortex (Alam et al. 1997; Ferrer 2009). Our results on protein carbonylation in mice brains indicate that there was an increase in oxidized

proteins in the striatum after treatment with both neurotoxin whereas at the hippocampal level the effect was less evident. The increase in carbonylation is statistically significant only for CysDA, however, 6-OHDA exerted a similar effect, and failed to reach statistical significance due to high standard deviation. Conversely to that observed in PD affected patients, in our model no protein carbonyls were detected in the prefrontal cortex. This difference may be justified by the selective lesion induced in the experimental model and by the timing of damage onset. Indeed, as already pointed out, neurodegeneration in PD is a slow process in which the impairment of neuronal function is the result of a progressive and continuous accumulation of damaged/disfunctioning molecules, contrary to what happens in the animal models, in which neuronal death is an acute event due to the fact that the neurotoxin is delivered in high amounts in a single shot at the striatal level.

Another characteristic feature of PD brains, directly related to oxidative stress, is the reduced GSH/GSSG ratio and the pronounced decrease of total GSH in brain specimens (Sofic et al. 1992). Here, we demonstrate that CysDA treatment induces GSH oxidation and depletion, and that this phenomenon is similar to that observed in PD affected patients where GSH oxidation does not seem to be accompanied by a corresponding increase of GSSG, which is formed in minor amount. Our data are also in good agreement with previous findings indicating an involvement of the GSH

cycle in the melanin-induced apoptotic death in SH-SY5Y cells, in which DA and synthetic pheomelanin showed a low concentration of GSH with respect to control (Naoi et al. 2008). It is notable that decreased a GSH level in the substantia nigra represents an early event in the pathological process that underlies PD (Martin and Teismann 2009). The question as to whether GSH depletion is due to oxidative stress or to alteration of its metabolic pathway still remains open. Some authors evidenced an alteration in the activity of key enzymes of the metabolism of GSH in PD brains, that was not confirmed in later work (Sian et al. 1994). However, there is an undoubted participation of the GSH/GSSG system in the response to the stress exerted by CysDA and in PD.

10.2 α-Synuclein expression and aggregation are prompted by CysDA treatment

Recent studies link oxidative stress to protein misfolding and to the Unfolded Protein Response (UPR) (Rao and Bredesen 2004; Holtz et al. 2006). Our data indicate that CysDA is able to perturb redox omeostasis of the cell thus possibly triggering protein misfolding, as evidenced by the increase in α-Syn aggregation. *In vivo* experiments demonstrated an increase

in α-Syn aggregated forms in the prefrontal cortex with both neurotoxins. These data are in agreement with previous findings which indicate that there is an involvement of the prefrontal cortex in Parkinson's disease (Ferrer 2009). In particular, an increase of the α-Syn dimeric form was evidenced in the prefrontal cortex with respect to the striatum. The dimeric form of the protein can be considered as a marker of oxidative stress and its formation is an essential step in α-Syn aggregation as demonstrated by Krishnan and colleagues (Krishnan et al. 2003). Indeed, the critical rate-limiting step in nucleation of α-Syn fibrils under physiological conditions is the oxidative formation and accumulation of the dimeric form linked via a dityrosine residue. This dimer is able to form a prenucleus that stimulates the aggregation of the protein. The evidence that oxidation is an essential step in α-Syn aggregation is supported by many findings indicating that different methionine oxidation, nitration and MDA-Lysine of α-Syn, are involved in the folding and aggregation in the different brain regions (Ferrer,2009).

Treatment of SH-SY5Y cells with both neurotoxins evidenced an increase of α-Syn protein level within 6 hours, that is consistent with the high mRNA level determined by qRT-PCR analysis. In the cytosol, both the dimeric and the monomeric forms of the protein were present, whereas in the nuclei only the monomeric form was detected, along with small amounts of oligomers. Previous work has demonstrated that α-Syn can form a stable

complex with histone H1, due to the significant presence of basic aminoacid residues in histone H1, which can electrostatically interact with the acidic C-terminal domain of α-Syn enriched in acidic residues (Goers et al. 2003). This interaction can dramatically accelerate fibrillation of the protein, giving rise to high molecular weight protofibrils and fibrils which cannot be detected and quantified by Western blot due to their extremely high molecular weight. The pathophysiological implications of this interaction are still not clarified, however, Goers and colleagues hypothesized that α-Syn-histone H1 complexes could have a regulatory role by decreasing the pool of free histones available for DNA binding, thus affecting transcriptional machinery (Goers et al. 2003).

10.3 Oxidative stress and the unfolded protein response

GSH is the major redox buffer of the ER lumen. An alteration of the thiol-disulfide redox buffer can impair the oxidative protein folding, causing the luminal accumulation of unfolded/misfolded proteins, which triggers the Unfolded Protein Response (UPR) and causes ER stress. Accumulating evidence suggests that ER stress induced by aberrant protein degradation is implicated in PD (Quan et al. 1995). The presence of ERp57 , one of the

proteins involved in ER stress, was evidenced in the brain of PD affected subjects (Wilhelmus et al. 2010). These authors demonstrated that ERp57 has a different staining pattern between PD subjects and aged-matched controls in melanized neurons of SN, i.e. a homogeneous cytoplasmic immunoreactivity in controls, and a granular distribution pattern in PD specimens. Notably, 6-OHDA was demonstrated to induce ERp57 upregulation in cultured neuronal cells including dopaminergic neurons, and was found to induce ROS-mediated UPR, which seems to initiate apoptosis via mitochondrial involvement (O'Malley et al. 2003; Holtz et al. 2006). Based on these results it has been hypothesized that ERp57 may play a role in 6-OHDA-mediated UPR induction.

Our results indicate that in mice treated with both CysDA and 6-OHDA there is an increase of ERp57 protein level in the striatum, the brain region directly involved in the lesion. Conversely, in the other brain areas, the level of this protein does not seem to be affected. Our data are in agreement with previous report which demonstrated that, after intracisternal administration of 6-OHDA in rats, there was an increase of ERp57 protein level in the striatum and midbrain 12h after treatment up to two weeks, indicating the induction of this protein (Akazawa et al. 2010). Treatment of SH-SY5Y cells with both neurotoxins evidenced an increase of ERp57 protein level within 3 hour, that is consistent with the high mRNA level

determined by qRT-PCR analysis, further supporting *in vivo* data.

The increased ERp57 level is a cellular response to oxidative stress exerted by the neurotoxins that induce perturbation of GSH/GSSG ratio. It can be speculated that in these conditions ERp57 may act as a chaperone to prevent protein misfolding and aggregation of α-Syn, as already hypothesized for Amyloid-beta peptide (Erickson et al. 2005).

In conclusion, our results demonstrate that CysDA exerts neurotoxic effects similar to 6-OHDA, supporting the hypothesis that CysDA may be an endogenous parkinsonian mimetic, able to induce α-Syn overexpression and aggregation, ER stress and consequent neurodegeneration.

11 Bibliography

Aiyar N., Bennett C. F., Nambi P., Valinski W., Angioli M., Minnich M. and Crooke S. T. (1989) Solubilization of rat liver vasopressin receptors as a complex with a guanine-nucleotide-binding protein and phosphoinositide-specific phospholipase C. Biochem J 261, 63-70.

Akazawa Y. O., Saito Y., Nishio K., Horie M., Kinumi T., Masuo Y., Yoshida Y., Ashida H. and Niki E. (2010) Proteomic characterization of the striatum and midbrain treated with 6-hydroxydopamine: alteration of 58-kDa glucose-regulated protein and C/EBP homologous protein. Free Radic Res 44, 410-421.

Alam Z. I., Daniel S. E., Lees A. J., Marsden D. C., Jenner P. and Halliwell B. (1997) A generalised increase in protein carbonyls in the brain in Parkinson's but not incidental Lewy body disease. J Neurochem 69, 1326-1329.

Altieri F., Grillo C., Maceroni M. and Chichiarelli S. (2008) DNA damage and repair: from molecular mechanisms to health implications. Antioxid Redox Signal 10, 891-937.

Altieri F., Maras B., Eufemi M., Ferraro A. and Turano C. (1993) Purification of a 57kDa nuclear matrix protein associated with thiol:protein-disulfide oxidoreductase and phospholipase C activities. Biochem Biophys Res Commun 194, 992-1000.

Banhegyi G., Mandl J. and Csala M. (2008) Redox-based endoplasmic reticulum dysfunction in neurological diseases. J Neurochem 107, 20-34.

Bennett C. F., Balcarek J. M., Varrichio A. and Crooke S. T. (1988) Molecular cloning and complete amino-acid sequence of form-I phosphoinositide-specific phospholipase C. Nature 334, 268-270.

Blandini F., Armentero M. T. and Martignoni E. (2008) The 6-hydroxydopamine model: news from the past. Parkinsonism Relat Disord 14 Suppl 2, S124-129.

Bourdi M., Demady D., Martin J. L., Jabbour S. K., Martin B. M., George J. W. and Pohl L. R. (1995) cDNA cloning and baculovirus expression of the human liver endoplasmic reticulum P58: characterization as a protein disulfide isomerase isoform, but not as a protease or a carnitine acyltransferase. Arch Biochem Biophys 323, 397-403.

Boyan B. D., Wong K. L., Fang M. and Schwartz Z. (2007) 1alpha,25(OH)2D3 is an autocrine regulator of extracellular matrix turnover and growth factor release via ERp60 activated matrix vesicle metalloproteinases. J Steroid Biochem Mol Biol 103, 467-472.

Branchi I., D'Andrea I., Armida M., Cassano T., Pezzola A., Potenza R. L., Morgese M. G., Popoli P. and Alleva E. (2008) Nonmotor symptoms in Parkinson's disease: investigating early-phase onset of behavioral dysfunction in the 6-hydroxydopamine-lesioned rat model. J Neurosci Res 86, 2050-2061.

Carstam R., Brinck C., Hindemith-Augustsson A., Rorsman H. and Rosengren E. (1991) The neuromelanin of the human substantia nigra. Biochim Biophys Acta 1097, 152-160.

Chen J., Olivares-Navarrete R., Wang Y., Herman T. R., Boyan B. D. and Schwartz Z. (2010) Protein-disulfide isomerase-associated 3 (Pdia3) mediates the membrane response to 1,25-dihydroxyvitamin D3 in osteoblasts. J Biol Chem 285, 37041-37050.

Cheng F. C., Kuo J. S., Chia L. G. and Dryhurst G. (1996) Elevated 5-S-cysteinyldopamine/homovanillic acid ratio and reduced homovanillic acid in cerebrospinal fluid: possible markers for and potential insights into the pathoetiology of Parkinson's disease. J Neural Transm 103, 433-446.

Chichiarelli S., Ferraro A., Altieri F., Eufemi M., Coppari S., Grillo C., Arcangeli V. and Turano C. (2007) The stress protein ERp57/GRP58 binds specific DNA sequences in HeLa cells. J Cell Physiol 210, 343-351.

Chioccara F. and Novellino E. (1986) A convenient one step synthesis of 5-Cystein-S-yldopa using ceric ammonium nitrate. Synthetic Commun 16, 967-971.

Coe H. and Michalak M. (2010) ERp57, a multifunctional endoplasmic reticulum resident oxidoreductase. Int J Biochem Cell Biol 42, 796-799.

Coe H., Jung J., Groenendyk J., Prins D. and Michalak M. (2009) ERp57 modulates STAT3 signaling from the lumen of the endoplasmic reticulum. J Biol Chem 285, 6725-6738.

Coe H., Jung J., Groenendyk J., Prins D. and Michalak M. (2010) ERp57 modulates STAT3 signaling from the lumen of the endoplasmic reticulum. J Biol Chem 285, 6725-6738.

Coppari S., Altieri F., Ferraro A., Chichiarelli S., Eufemi M. and Turano C. (2002) Nuclear localization and DNA interaction of protein disulfide isomerase ERp57 in mammalian cells. J Cell Biochem 85, 325-333.

Corazzari M., Lovat P. E., Armstrong J. L., Fimia G. M., Hill D. S., Birch-Machin M., Redfern C. P. and Piacentini M. (2007) Targeting

homeostatic mechanisms of endoplasmic reticulum stress to increase susceptibility of cancer cells to fenretinide-induced apoptosis: the role of stress proteins ERdj5 and ERp57. Br J Cancer 96, 1062-1071.

Crawford G. E., Holt I. E., Mullikin J. C., Tai D., Blakesley R., Bouffard G., Young A., Masiello C., Green E. D., Wolfsberg T. G. and Collins F. S. (2004) Identifying gene regulatory elements by genome-wide recovery of DNase hypersensitive sites. Proc Natl Acad Sci U S A 101, 992-997.

Dauer W. and Przedborski S. (2003) Parkinson's disease: mechanisms and models. Neuron 39, 889-909.

Degen E. and Williams D. B. (1991) Participation of a novel 88-kD protein in the biogenesis of murine class I histocompatibility molecules. J Cell Biol 112, 1099-1115.

Dittmer J. (2003) The biology of the Ets1 proto-oncogene. Mol Cancer 2, 29.

Dong L., Jiang C. C., Thorne R. F., Croft A., Yang F., Liu H., de Bock C. E., Hersey P. and Zhang X. D. (2011) Ets-1 mediates upregulation of Mcl-1 downstream of XBP-1 in human melanoma cells upon ER stress. Oncogene 30, 3716-3726.

Erickson R. R., Dunning L. M., Olson D. A., Cohen S. J., Davis A. T., Wood W. G., Kratzke R. A. and Holtzman J. L. (2005) In cerebrospinal fluid ER chaperones ERp57 and calreticulin bind beta-amyloid. Biochem Biophys Res Commun 332, 50-57.

Eufemi M., Coppari S., Altieri F., Grillo C., Ferraro A. and Turano C. (2004) ERp57 is present in STAT3-DNA complexes. Biochem Biophys Res Commun 323, 1306-1312.

Fahn S. and Cohen G. (1992) The oxidant stress hypothesis in Parkinson's disease: evidence supporting it. Ann Neurol 32, 804-812.

Ferrer I. (2009) Early involvement of the cerebral cortex in Parkinson's disease: convergence of multiple metabolic defects. Prog Neurobiol 88, 89-103.

Freedman R. B., Hirst T. R. and Tuite M. F. (1994) Protein disulphide isomerase: building bridges in protein folding. Trends Biochem Sci 19, 331-336.

Frickel E. M., Frei P., Bouvier M., Stafford W. F., Helenius A., Glockshuber R. and Ellgaard L. (2004) ERp57 is a multifunctional thiol-disulfide oxidoreductase. J Biol Chem 279, 18277-18287.

Garbi N., Tanaka S., Momburg F. and Hammerling G. J. (2006) Impaired assembly of the major histocompatibility complex class I peptide-loading complex in mice deficient in the oxidoreductase ERp57. Nat Immunol 7, 93-102.

Goers J., Manning-Bog A. B., McCormack A. L., Millett I. S., Doniach S., Di Monte D. A., Uversky V. N. and Fink A. L. (2003) Nuclear localization of alpha-synuclein and its interaction with histones. Biochemistry 42, 8465-8471.

Grillo C., D'Ambrosio C., Scaloni A., Maceroni M., Merluzzi S., Turano C. and Altieri F. (2006) Cooperative activity of Ref-1/APE and ERp57 in reductive activation of transcription factors. Free Radic Biol Med 41, 1113-1123.

Grillo C., D'Ambrosio C., Consalvi V., Chiaraluce R., Scaloni A., Maceroni M., Eufemi M. and Altieri F. (2007) DNA-binding activity of the ERp57 C-terminal domain is related to a redox-dependent conformational change. J Biol Chem 282, 10299-10310.

Grindel B. J., Rohe B., Safford S. E., Bennett J. J. and Farach-Carson M. C. (2011) Tumor necrosis factor-alpha treatment of HepG2 cells mobilizes a cytoplasmic pool of ERp57/1,25D-MARRS to the nucleus. J Cell Biochem 112, 2606-2615.

Gross D. S. and Garrard W. T. (1988) Nuclease hypersensitive sites in chromatin. Annu Rev Biochem 57, 159-197.

Guo G. G., Patel K., Kumar V., Shah M., Fried V. A., Etlinger J. D. and Sehgal P. B. (2002) Association of the chaperone glucose-regulated protein 58 (GRP58/ER-60/ERp57) with Stat3 in cytosol and plasma membrane complexes. J Interferon Cytokine Res 22, 555-563.

Feng J, Villeponteau B. (1992). High resolution analysis of c-fos chromatin accessibility using a novel DNase I-PCR assay. Biochim Biophys Acta 1130:253–258.

Hahne J. C., Okuducu A. F., Sahin A., Fafeur V., Kiriakidis S. and Wernert N. (2008) The transcription factor ETS-1: its role in tumour development and strategies for its inhibition. Mini Rev Med Chem 8, 1095-1105.

Hanein S., Perrault I., Roche O., Gerber S., Khadom N., Rio M., Boddaert N., Jean-Pierre M., Brahimi N., Serre V., Chretien D., Delphin N., Fares-Taie L., Lachheb S., Rotig A., Meire F., Munnich A., Dufier J. L., Kaplan J. and Rozet J. M. (2009) TMEM126A, encoding a mitochondrial protein, is mutated in autosomal-recessive nonsyndromic optic atrophy. Am J Hum Genet 84, 493-498.

Hetz C., Russelakis-Carneiro M., Walchli S., Carboni S., Vial-Knecht E., Maundrell K., Castilla J. and Soto C. (2005) The disulfide isomerase Grp58 is a protective factor against prion neurotoxicity. J Neurosci 25, 2793-2802.

Hirano N., Shibasaki F., Sakai R., Tanaka T., Nishida J., Yazaki Y., Takenawa T. and Hirai H. (1995) Molecular cloning of the human glucose-regulated protein ERp57/GRP58, a thiol-dependent reductase.

Identification of its secretory form and inducible expression by the oncogenic transformation. Eur J Biochem 234, 336-342.
Hissin P. J. and Hilf R. (1976) A fluorometric method for determination of oxidized and reduced glutathione in tissues. Anal Biochem 74, 214-226.
Holtz W. A. and O'Malley K. L. (2003) Parkinsonian mimetics induce aspects of unfolded protein response in death of dopaminergic neurons. J Biol Chem 278, 19367-19377.
Holtz W. A., Turetzky J. M., Jong Y. J. and O'Malley K. L. (2006) Oxidative stress-triggered unfolded protein response is upstream of intrinsic cell death evoked by parkinsonian mimetics. J Neurochem 99, 54-69.
Kelley M. R. and Parsons S. H. (2001) Redox regulation of the DNA repair function of the human AP endonuclease Ape1/ref-1. Antioxid Redox Signal 3, 671-683.
Khanal R. C. and Nemere I. (2007) The ERp57/GRp58/1,25D3-MARRS receptor: multiple functional roles in diverse cell systems. Curr Med Chem 14, 1087-1093.
Kim-Han J. S. and O'Malley K. L. (2007) Cell stress induced by the parkinsonian mimetic, 6-hydroxydopamine, is concurrent with oxidation of the chaperone, ERp57, and aggresome formation. Antioxid Redox Signal 9, 2255-2264.
Koivunen P., Horelli-Kuitunen N., Helaakoski T., Karvonen P., Jaakkola M., Palotie A. and Kivirikko K. I. (1997) Structures of the human gene for the protein disulfide isomerase-related polypeptide ERp60 and a processed gene and assignment of these genes to 15q15 and 1q21. Genomics 42, 397-404.
Kozlov G., Maattanen P., Schrag J. D., Pollock S., Cygler M., Nagar B., Thomas D. Y. and Gehring K. (2006) Crystal structure of the bb' domains of the protein disulfide isomerase ERp57. Structure 14, 1331-1339.
Krishnan S., Chi E. Y., Wood S. J., Kendrick B. S., Li C., Garzon-Rodriguez W., Wypych J., Randolph T. W., Narhi L. O., Biere A. L., Citron M. and Carpenter J. F. (2003) Oxidative dimer formation is the critical rate-limiting step for Parkinson's disease alpha-synuclein fibrillogenesis. Biochemistry 42, 829-837.
Krynetskaia N. F., Phadke M. S., Jadhav S. H. and Krynetskiy E. Y. (2009) Chromatin-associated proteins HMGB1/2 and PDIA3 trigger cellular response to chemotherapy-induced DNA damage. Mol Cancer Ther 8, 864-872.
Krynetski E. Y., Krynetskaia N. F., Bianchi M. E. and Evans W. E. (2003) A nuclear protein complex containing high mobility group proteins B1 and

B2, heat shock cognate protein 70, ERp60, and glyceraldehyde-3-phosphate dehydrogenase is involved in the cytotoxic response to DNA modified by incorporation of anticancer nucleoside analogues. Cancer Res 63, 100-106.

Leach M. R., Cohen-Doyle M. F., Thomas D. Y. and Williams D. B. (2002) Localization of the lectin, ERp57 binding, and polypeptide binding sites of calnexin and calreticulin. J Biol Chem 277, 29686-29697.

Lee A. S. (2001) The glucose-regulated proteins: stress induction and clinical applications. Trends Biochem Sci 26, 504-510.

Li Y. and Camacho P. (2004) Ca2+-dependent redox modulation of SERCA 2b by ERp57. J Cell Biol 164, 35-46.

Lindquist J. A., Jensen O. N., Mann M. and Hammerling G. J. (1998) ER-60, a chaperone with thiol-dependent reductase activity involved in MHC class I assembly. Embo J 17, 2186-2195.

Mah S. J., Ades A. M., Mir R., Siemens I. R., Williamson J. R. and Fluharty S. J. (1992) Association of solubilized angiotensin II receptors with phospholipase C-alpha in murine neuroblastoma NIE-115 cells. Mol Pharmacol 42, 217-226.

Markus M. and Benezra R. (1999) Two isoforms of protein disulfide isomerase alter the dimerization status of E2A proteins by a redox mechanism. J Biol Chem 274, 1040-1049.

Martin H. L. and Teismann P. (2009) Glutathione--a review on its role and significance in Parkinson's disease. Faseb J 23, 3263-3272.

Martin S. A., Lord C. J. and Ashworth A. (2010) Therapeutic targeting of the DNA mismatch repair pathway. Clin Cancer Res 16, 5107-5113.

Martin V., Groenendyk J., Steiner S. S., Guo L., Dabrowska M., Parker J. M., Muller-Esterl W., Opas M. and Michalak M. (2006) Identification by mutational analysis of amino acid residues essential in the chaperone function of calreticulin. J Biol Chem 281, 2338-2346.

Mazzio E. A., Close F. and Soliman K. F. (2011) The biochemical and cellular basis for nutraceutical strategies to attenuate neurodegeneration in Parkinson's disease. Int J Mol Sci 12, 506-569.

Miller R. L., James-Kracke M., Sun G. Y. and Sun A. Y. (2009) Oxidative and inflammatory pathways in Parkinson's disease. Neurochem Res 34, 55-65.

Mosca L., Tempera I., Lendaro E., Di Francesco L. and d'Erme M. (2008) Characterization of catechol-thioether-induced apoptosis in human SH-SY5Y neuroblastoma cells. J Neurosci Res 86, 954-960.

Mosca L., Lendaro E., d'Erme M., Marcellini S., Moretti S. and Rosei M. A. (2006) 5-S-Cysteinyl-dopamine effect on the human dopaminergic neuroblastoma cell line SH-SY5Y. Neurochem Int 49, 262-269.

Murray J. I., Whitfield M. L., Trinklein N. D., Myers R. M., Brown P. O. and Botstein D. (2004) Diverse and specific gene expression responses to stresses in cultured human cells. Mol Biol Cell 15, 2361-2374.

Naoi M., Maruyama W., Yi H., Yamaoka Y., Shamoto-Nagai M., Akao Y., Gerlach M., Tanaka M. and Riederer P. (2008) Neuromelanin selectively induces apoptosis in dopaminergic SH-SY5Y cells by deglutathionylation in mitochondria: involvement of the protein and melanin component. J Neurochem 105, 2489-2500.

Nardo G., Pozzi S., Pignataro M., Lauranzano E., Spano G., Garbelli S., Mantovani S., Marinou K., Papetti L., Monteforte M., Torri V., Paris L., Bazzoni G., Lunetta C., Corbo M., Mora G., Bendotti C. and Bonetto V. (2011) Amyotrophic lateral sclerosis multiprotein biomarkers in peripheral blood mononuclear cells. PLoS One 6, e25545.

Ndubuisi M. I., Guo G. G., Fried V. A., Etlinger J. D. and Sehgal P. B. (1999) Cellular physiology of STAT3: Where's the cytoplasmic monomer? J Biol Chem 274, 25499-25509.

Nemere I., Garbi N., Hammerling G. J. and Khanal R. C. (2010) Intestinal cell calcium uptake and the targeted knockout of the 1,25D3-MARRS (membrane-associated, rapid response steroid-binding) receptor/PDIA3/Erp57. J Biol Chem 285, 31859-31866.

Nemere I., Farach-Carson M. C., Rohe B., Sterling T. M., Norman A. W., Boyan B. D. and Safford S. E. (2004) Ribozyme knockdown functionally links a 1,25(OH)2D3 membrane binding protein (1,25D3-MARRS) and phosphate uptake in intestinal cells. Proc Natl Acad Sci U S A 101, 7392-7397.

O'Malley K. L., Liu J., Lotharius J. and Holtz W. (2003) Targeted expression of BCL-2 attenuates MPP+ but not 6-OHDA induced cell death in dopaminergic neurons. Neurobiol Dis 14, 43-51.

Ohtani H., Wakui H., Ishino T., Komatsuda A. and Miura A. B. (1993) An isoform of protein disulfide isomerase is expressed in the developing acrosome of spermatids during rat spermiogenesis and is transported into the nucleus of mature spermatids and epididymal spermatozoa. Histochemistry 100, 423-429.

Olanow C. W. and Tatton W. G. (1999) Etiology and pathogenesis of Parkinson's disease. Annu Rev Neurosci 22, 123-144.

Oliver J. D., van der Wal F. J., Bulleid N. J. and High S. (1997) Interaction of the thiol-dependent reductase ERp57 with nascent glycoproteins. Science 275, 86-88.

Oliver J. D., Roderick H. L., Llewellyn D. H. and High S. (1999) ERp57 functions as a subunit of specific complexes formed with the ER lectins calreticulin and calnexin. Mol Biol Cell 10, 2573-2582.

Ozaki T., Yamashita T. and Ishiguro S. (2008) ERp57-associated mitochondrial micro-calpain truncates apoptosis-inducing factor. Biochim Biophys Acta 1783, 1955-1963.

Pamer E. and Cresswell P. (1998) Mechanisms of MHC class I--restricted antigen processing. Annu Rev Immunol 16, 323-358.

Perez R. G. and Hastings T. G. (2004) Could a loss of alpha-synuclein function put dopaminergic neurons at risk? J Neurochem 89, 1318-1324.

Pollock S., Kozlov G., Pelletier M. F., Trempe J. F., Jansen G., Sitnikov D., Bergeron J. J., Gehring K., Ekiel I. and Thomas D. Y. (2004) Specific interaction of ERp57 and calnexin determined by NMR spectroscopy and an ER two-hybrid system. Embo J 23, 1020-1029.

Ramirez-Rangel I., Bracho-Valdes I., Vazquez-Macias A., Carretero-Ortega J., Reyes-Cruz G. and Vazquez-Prado J. Regulation of mTORC1 complex assembly and signaling by GRp58/ERp57. Mol Cell Biol 31, 1657-1671.

Rao R. V. and Bredesen D. E. (2004) Misfolded proteins, endoplasmic reticulum stress and neurodegeneration. Curr Opin Cell Biol 16, 653-662.

Ray S., Lee C., Hou T., Bhakat K. K. and Brasier A. R. (2010) Regulation of signal transducer and activator of transcription 3 enhanceosome formation by apurinic/apyrimidinic endonuclease 1 in hepatic acute phase response. Mol Endocrinol 24, 391-401.

Reiter R. J., Manchester L. C. and Tan D. X. (2010) Neurotoxins: free radical mechanisms and melatonin protection. Curr Neuropharmacol 8, 194-210.

Rosengren E., Linder-Eliasson E. and Carlsson A. (1985) Detection of 5-S-cysteinyldopamine in human brain. J Neural Transm 63, 247-253.

Salauze L., van der Velden C., Lagroye I., Veyret B. and Geffard M. (2005) Circulating antibodies to cysteinyl catecholamines in amyotrophic lateral sclerosis and Parkinson's disease patients. Amyotroph Lateral Scler Other Motor Neuron Disord 6, 226-233.

Sambrook J, Russel DW. 2001. Molecular cloning. Cold Spring Harbor, New York: Cold Spring Harbor Laboratory Press.

Schelhaas M., Malmstrom J., Pelkmans L., Haugstetter J., Ellgaard L., Grunewald K. and Helenius A. (2007) Simian Virus 40 depends on ER protein folding and quality control factors for entry into host cells. Cell 131, 516-529.

Schultz-Norton J. R., McDonald W. H., Yates J. R. and Nardulli A. M. (2006) Protein disulfide isomerase serves as a molecular chaperone to

maintain estrogen receptor alpha structure and function. Mol Endocrinol 20, 1982-1995.

Sehgal P. B., Guo G. G., Shah M., Kumar V. and Patel K. (2002) Cytokine signaling: STATS in plasma membrane rafts. J Biol Chem 277, 12067-12074.

Sian J., Dexter D. T., Lees A. J., Daniel S., Agid Y., Javoy-Agid F., Jenner P. and Marsden C. D. (1994) Alterations in glutathione levels in Parkinson's disease and other neurodegenerative disorders affecting basal ganglia. Ann Neurol 36, 348-355.

Sidell K. R., Olson S. J., Ou J. J., Zhang Y., Amarnath V. and Montine T. J. (2001) Cysteine and mercapturate conjugates of oxidized dopamine are in human striatum but only the cysteine conjugate impedes dopamine trafficking in vitro and in vivo. J Neurochem 79, 510-521.

Sofic E., Lange K. W., Jellinger K. and Riederer P. (1992) Reduced and oxidized glutathione in the substantia nigra of patients with Parkinson's disease. Neurosci Lett 142, 128-130.

Spencer J. P., Whiteman M., Jenner P. and Halliwell B. (2002) 5-s-Cysteinyl-conjugates of catecholamines induce cell damage, extensive DNA base modification and increases in caspase-3 activity in neurons. J Neurochem 81, 122-129.

Storch A., Ludolph A. C. and Schwarz J. (2004) Dopamine transporter: involvement in selective dopaminergic neurotoxicity and degeneration. J Neural Transm 111, 1267-1286.

Sultana R., Perluigi M. and Butterfield D. A. (2009) Oxidatively modified proteins in Alzheimer's disease (AD), mild cognitive impairment and animal models of AD: role of Abeta in pathogenesis. Acta Neuropathol 118, 131-150.

Tian G., Xiang S., Noiva R., Lennarz W. J. and Schindelin H. (2006) The crystal structure of yeast protein disulfide isomerase suggests cooperativity between its active sites. Cell 124, 61-73.

Tourkova I. L., Shurin G. V., Chatta G. S., Perez L., Finke J., Whiteside T. L., Ferrone S. and Shurin M. R. (2005) Restoration by IL-15 of MHC class I antigen-processing machinery in human dendritic cells inhibited by tumor-derived gangliosides. J Immunol 175, 3045-3052.

Tunsophon S. and Nemere I. (2010) Protein kinase C isotypes in signal transduction for the 1,25D3-MARRS receptor (ERp57/PDIA3) in steroid hormone-stimulated phosphate uptake. Steroids 75, 307-313.

Turano C., Gaucci E., Grillo C. and Chichiarelli S. (2011) ERp57/GRP58: a protein with multiple functions. Cell Mol Biol Lett 16, 539-563.

Urade R., Okudo H., Kato H., Moriyama T. and Arakaki Y. (2004) ER-60 domains responsible for interaction with calnexin and calreticulin. Biochemistry 43, 8858-8868.

Venda L. L., Cragg S. J., Buchman V. L. and Wade-Martins R. (2010) alpha-Synuclein and dopamine at the crossroads of Parkinson's disease. Trends Neurosci 33, 559-568.

Wang H. Q. and Takahashi R. (2007) Expanding insights on the involvement of endoplasmic reticulum stress in Parkinson's disease. Antioxid Redox Signal 9, 553-561.

Wearsch P. A. and Cresswell P. (2008) The quality control of MHC class I peptide loading. Curr Opin Cell Biol 20, 624-631.

Wilhelmus M. M., Verhaar R., Andringa G., Bol J. G., Cras P., Shan L., Hoozemans J. J. and Drukarch B. (2010) Presence of tissue transglutaminase in granular endoplasmic reticulum is characteristic of melanized neurons in Parkinson's disease brain. Brain Pathol 21, 130-139.

Wilhelmus M. M., Verhaar R., Andringa G., Bol J. G., Cras P., Shan L., Hoozemans J. J. and Drukarch B. (2011) Presence of tissue transglutaminase in granular endoplasmic reticulum is characteristic of melanized neurons in Parkinson's disease brain. Brain Pathol 21, 130-139.

Wu W., Beilhartz G., Roy Y., Richard C. L., Curtin M., Brown L., Cadieux D., Coppolino M., Farach-Carson M. C., Nemere I. and Meckling K. A. (2010) Nuclear translocation of the 1,25D3-MARRS (membrane associated rapid response to steroids) receptor protein and NFkappaB in differentiating NB4 leukemia cells. Exp Cell Res 316, 1101-1108.

Xanthoudakis S. and Curran T. (1992) Identification and characterization of Ref-1, a nuclear protein that facilitates AP-1 DNA-binding activity. Embo J 11, 653-665.

Xie H. R., Hu L. S. and Li G. Y. (2010) SH-SY5Y human neuroblastoma cell line: in vitro cell model of dopaminergic neurons in Parkinson's disease. Chin Med J (Engl) 123, 1086-1092.

Yacoub A., Kelley M. R. and Deutsch W. A. (1997) The DNA repair activity of human redox/repair protein APE/Ref-1 is inactivated by phosphorylation. Cancer Res 57, 5457-5459.

Zapun A., Darby N. J., Tessier D. C., Michalak M., Bergeron J. J. and Thomas D. Y. (1998) Enhanced catalysis of ribonuclease B folding by the interaction of calnexin or calreticulin with ERp57. J Biol Chem 273, 6009-6012.

Zecca L., Tampellini D., Gerlach M., Riederer P., Fariello R. G. and Sulzer D. (2001) Substantia nigra neuromelanin: structure, synthesis, and molecular behaviour. Mol Pathol 54, 414-418.

Zhang F. and Dryhurst G. (1994) Effects of L-cysteine on the oxidation chemistry of dopamine: new reaction pathways of potential relevance to idiopathic Parkinson's disease. J Med Chem 37, 1084-1098.

Zhang Y., Kozlov G., Pocanschi C. L., Brockmeier U., Ireland B. S., Maattanen P., Howe C., Elliott T., Gehring K. and Williams D. B. (2009) ERp57 does not require interactions with calnexin and calreticulin to promote assembly of class I histocompatibility molecules, and it enhances peptide loading independently of its redox activity. J Biol Chem 284, 10160-10173.

Zhu L., Santos N. C. and Kim K. H. (2010) Disulfide isomerase glucose-regulated protein 58 is required for the nuclear localization and degradation of retinoic acid receptor alpha. Reproduction 139, 717-731.

Zucca F. A., Giaveri G., Gallorini M., Albertini A., Toscani M., Pezzoli G., Lucius R., Wilms H., Sulzer D., Ito S., Wakamatsu K. and Zecca L. (2004) The neuromelanin of human substantia nigra: physiological and pathogenic aspects. Pigment Cell Res 17, 610-617.

12 Attachments

Manuscript
Click here to download Manuscript: Aureli_MolCellBiochem.doc Click here to view linked References

ERp57 is a potential transcriptional regulatory factor for genes involved in the stress response

Aureli Cristina[1]*, Gaucci Elisa[1]*, Arcangeli Valentina, Grillo Caterina[1,2], Eufemi Margherita[1,2] and Silvia Chichiarelli[1§]

[1]Department of Biochemical Sciences "A. Rossi Fanelli", "Sapienza" University of Rome, Piazzale Aldo Moro 5, Rome 00185, Italy

[2]Istituto Pasteur-Fondazione Cenci Bolognetti, "Sapienza" University of Rome, Piazzale Aldo Moro 5, Rome 00185, Italy

*contributed equally

[§]Corresponding author: Silvia Chichiarelli;
E-mail address: silvia.chichiarelli@uniroma1.it
Tel.: +39 06 49910945; Fax: +39 06 4440062

Abstract

ERp57/PDIA3 is a ubiquitously expressed disulfide isomerase protein, which acts in concert with the lectins calreticulin and calnexin in the folding of glycoproteins destined to the plasma membrane or to be secreted. Its canonical compartment is the endoplasmic reticulum, where it acts as chaperone and redox catalyst, but non canonical locations have been described as well. One of these is the nucleus, where ERp57 has been found associated with DNA and nuclear proteins. In a previous work performed in HeLa cells, ERp57 has been demonstrated to bind specific DNA sequences involved in the stress response. The direct interaction with the DNA sequences identified as ERp57-targeted regions in HeLa cells has now been confirmed in a melanoma cell line. Furthermore, the ERp57 silencing, achieved by RNA interference, has produced a significant down-modulation of the target genes expression. The possible involvement of other proteins in complex with ERp57 has been studied by an *in vitro* biotin-streptavidin based binding assay and the interacting protein APE/Ref-1 has been also assessed for its direct association with the ERp57 target regions. In conclusion, nuclear ERp57 interacts *in vivo* with DNA fragments in melanoma cells and is potentially involved in the transcriptional regulation of its target genes.

Keywords

ERp57/PDIA3; transcriptional regulation; chromatin immunoprecipitation; RNA interference; MSH6; APE/Ref-1

1. Introduction

The protein ERp57/PDIA3, member of the protein disulfide isomerase family and mainly located in the endoplasmic reticulum (ER), shares a thiol-disulfide exchange activity with other family members. It is involved in the proper folding and in the formation and reshuffling of the disulfide bridges of the proteins synthesized in the rough ER, destined to be secreted or incorporated in the cell membrane [1]. Therefore its function, which is essential for cell viability, is that of chaperone and redox-catalyst, this latter activity being due to its reshuffling of the disulfide bridges [2-4]. Considering these functions, it is not surprising that the expression of ERp57 is usually up-regulated under stress conditions [5]. In this context, it has recently emerged that ER stress induced by misfolded prions is accompanied by ERp57 overexpression [6].

ERp57 shows a ubiquitous distribution in a wide variety of cell types, even outside its canonical compartment [7, 8]. In the cytosol it has been found associated with other proteins. In this location it acts as component of a multiprotein complex [9], being required for the activation and transcriptional activity of STAT3 [10]. The association of ERp57 with STAT3 has also been found in the lipid raft fraction of the cell membrane [11]. Moreover, together with calreticulin, ERp57 appears at the surface of cells that are treated with immunogenic cell death inducers [12].

A nuclear localization of ERp57 has been suggested for the first time by gel shift experiments showing that this protein alters the formation of complexes between nuclear proteins and the regulatory domain of interferon-inducible genes [13]. The protein has been previously found in the nuclei of rat spermatids and spermatozoa [14] and in human blood cells [15]. Subsequently, the presence of ERp57 in the internal nuclear matrix was demonstrated in preparations from 3T3 and HeLa cells and the protein has been found in complex with DNA by two agents of cross-linking, cis-diamminedichloro platinum II (cis-DDP) and formaldehyde, in the same type of cells [16].

A hypothesis for the role of nuclear ERp57 can be made about the reduction and activation of transcription factors. In fact, a regulatory activity of ERp57 on the redox state and functional properties of the transcription factor E2A has been described [17].

The findings by Krynetski et al. [18] that ERp57 is present in a multiprotein complex capable of detecting changes in DNA structure suggest that ERp57 might take an active part also in the DNA repair process. This hypothesis is further corroborated by the association with the human apurinic/apyrimidinic endonuclease (APE/Ref-1) [19], which is a dual-function protein that has important roles in the repair of baseless sites that arise in DNA and in regulating the redox state of a number of proteins [20].

The finding that, in HeLa cells, ERp57 binds a number of genes involved in the stress response and in the oxidative phosphorylation [21] enables to delineate the correlation between the stress-response and the nuclear location of ERp57, as well as its possible role as transcription factor. In

this context, the aim of the present work was to clarify the role of the nuclear ERp57 in a melanoma cell line, focusing on its involvement in gene regulation. First of all, the direct interaction with the DNA sequences identified as ERp57 target regions in HeLa cells was searched in M14 cells by means of chromatin immunoprecipitation (ChIP). Next, we have exploited a RNA interference (RNAi) strategy to silence the expression of ERp57 in the cells and the expression levels of its potential target genes have been evaluated by Real Time PCR. An *in vitro* binding assay has been then performed to investigate the interaction of proteins potentially related to ERp57 at the level of its DNA target regions. Finally, ChIP assays have been carried out to study the *in vivo* binding of the protein APE/Ref-1 to the ERp57 target regions.

2. Materials and methods

2.1 Cell culture

Human melanoma (M14) cells were grown to 70-80% confluence at 37°C in an atmosphere of 5% CO_2 in RPMI medium, supplemented with 10% foetal bovine serum, 1% w/v sodium pyruvate, 2 mM glutamine, 100 U/ml of penicillin and 100 µg/ml of streptomycin. The cell culture reagents were supplied by PAA.

2.2 Cross-linking by cis-diamminedichloro platinum (cis-DDP) and ChIP

Experiments of chromatin immunoprecipitation (ChIP) were performed in M14 cells after a step of DNA-protein cross-linking by cis-diamminedichloro platinum II (cis-DDP, Sigma), as previously described [21,22]. The DNA-protein complexes, after a pre-clearing step, were split in two equal aliquots, hereafter named Sample (S) and mock (C). The Sample was incubated with a polyclonal anti-ERp57 antibody purified in our lab from rabbit serum or alternatively with a rabbit polyclonal anti-APE/Ref-1 antibody (Santa Cruz), while the mock was incubated with total IgG purified from preimmune rabbit serum (Sigma). The DNA fragments from Sample and mock immunoprecipitations were amplified with clone-specific primers to analyze the enrichment of the same DNA sequences in the Sample compared to the mock. We designed the clone-specific primers (see Table I –Supplementary Material) by the use of Primer3 (Whitehead Institute for Biomedical Research). Each clone was amplified by PCR with Jumpstart REDAccuTaq (Sigma) and a Perkin Elmer thermal Cycler 2400, using the following program steps: denaturation (96°C for 1 min), amplification repeated 30 times (94°C for 15 s, 55°C for 1 min, 68°C for 2 min) and extension (68°C for 10 min).

2.3 RNAi silencing of the protein ERp57

The silencing of the protein ERp57 in M14 cells was obtained by the administration of specific siRNA (Hs_GRP58_6_HP Validated siRNA, QIAGEN). The day before transfection, 2.5 x 10^4 cells per well of a 96-well plate in 100 µl of a complete culture medium (containing serum and antibiotics) were seeded. The siRNA was used at 0.3 µg/µl final concentration and Lipofectamine™ RNAiMAX (Invitrogen) was used as transfection agent. The transfection was carried out according to the manufacturer's instructions. M14 cells were incubated with the transfection complexes under their normal growth conditions and gene expression was monitored at the mRNA level after 48 h. Cells treated with scrambled, non-specific siRNA duplex (AllStars Negative control siRNA, QIAGEN) were used as control reference to exclude any nonspecific effect due to the treatment.

2.4 Total RNA extraction and cDNA synthesis

Cells were harvested and the total RNA was isolated with TRIzol Reagent (Invitrogen) following the manufacturer's instructions. RNA was precipitated by adding isopropanol, washed with 75% ethanol and dried air. The total RNA was resuspended in sterile RNase-free water and subjected to reverse transcription.

The reverse transcription of total RNA was conducted with SideStep™ II QPCR cDNA Synthesis Kit (Stratagene), according to the manufacturer's instructions.

2.5 Real Time PCR

ERp57, MSH6, TMEM126A, LRBA and ETS1 cDNA expression was evaluated with specific primers (QuantiTect® QIAGEN) by Real-Time PCR (RT-PCR), which was performed using a MJ MiniOpticon Detection System (BioRad Laboratories, Ltd) by means of Brilliant® SYBR® Green QPCR Master Mix (Stratagene). The protocol used was: denaturation (95°C for 5 min), amplification repeated 40 times (95°C for 30 s, 55°C for 30 s, 72°C for 30 s). A melting curve was performed following every run to ensure a single amplified product for every reaction: PCR fluorophore acquisition temperatures were set from 40°C to 95°C, reading every 0.5°C. All reactions were carried out in at least duplicate. RPS27A (QuantiTect® QIAGEN) was used as reference for normalization and the relative quantification was analysed using Gene Expression Analysis for iCycler iQ Real Time PCR Detection System Software, Version 1.10 (BioRad Laboratories, Ltd).

2.6 Nuclei purification and nuclear extract preparation

M14 cells were harvested by scraping in PBS and were resuspended in a hypotonic lysis buffer [10 mM Hepes, pH 8, 10 mM KCl, 1.5 mM $MgCl_2$, 30 mM sucrose, 0.5 mM dithiothreitol (DTT),

supplemented with an inhibitor cocktail (1 mM phenylmethylsulfonyl fluoride, 10 µM amido-phenylmethyl sulfonyl fluoride; 0.2 mM L-1-chloro-3-(4-tosylamido)-4-phenyl-2-butanone, 0.15 µM aprotinin, 1 µg/ml E64, 1 µM pepstatin)] by using a hypodermic needle. The suspension was incubated on ice for 10 min and then centrifuged at 1,400 g for 10 min at 4°C. The nuclei pellet was resuspended again in the lysis buffer, supplemented with 0.05% Triton X-100, and incubated on ice for 10 min. After centrifuging, the pellet was washed three times with lysis buffer supplemented with 1 mM $CaCl_2$.

The nuclear extract was obtained by treating the purified nuclei with NE buffer (20 mM Hepes, pH 8, 10 mM KCl, 0.42 M NaCl, 20% glycerol and the inhibitor cocktail) for 30 min on ice. After the incubation, the suspension was centrifuged at 10,000 g for 20 min at 4°C and the supernatant, containing the nuclear extract, was collected. The extraction was repeated again on the pellet and the two supernatants were joined.

2.7 Amplification of the biotinylated DNA fragments

The amplification of the biotinylated sequences of MSH6, TMEM126A, ETS1 and LRBA was performed using total DNA from M14 cells and Jumpstart REDAccuTaq (Sigma). A Perkin Elmer thermal Cycler 2400 was utilized for the PCR amplification and the protocol used was the following: denaturation (96°C for 1 min), amplification repeated 30 times (94°C for 15 s, 57°C for 1 min, 68°C for 2 min) and extension (68°C for 10 min). The amplification generated a single band displaying the predicted size. The amplified DNA fragment was purified with a commercial kit (QIAEX® II Gel extraction kit, QIAGEN).

2.8 In vitro binding assay

Streptavidin-coated magnetic beads (Dynal, Invitrogen) were washed three times in buffer A (5 mM Tris–HCl, pH 7.5, 0.5 mM EDTA, 1 M NaCl) using a magnetic separator (Dynal, Invitrogen). The biotinylated DNA fragments, corresponding to MSH6, ETS1, LRBA or TMEM126A genes, were incubated with the beads for 2 h at 4°C in buffer A (Sample). Control experiments were carried out by using streptavidin-beads saturated with biotin (Control). Sample and Control beads were then incubated with 10 nM biotin in buffer A for 30 min at 4°C and washed three times in buffer A. Subsequently, Sample and Control beads were incubated with 0.5% BSA in buffer A for 30 min at 4°C, then washed three times in buffer A and once in buffer B (20 mM Tris–HCl, pH 8, 5 mM EDTA, 5% glycerol, 0.1% Nonidet P40 and the protease inhibitor cocktail). The nuclear extract from M14 cells was diluted in buffer B to 50 mM NaCl and pre-incubated for 5 min with E. coli DNA (Sigma), which was used as competitor in a 500-fold excess in respect to the immobilized DNA. The nuclear extract was then split in two equal aliquots and mixed with Sample or Control beads, incubating o.n. at 4°C in gentle rotation. The day after, the beads were washed four times in

buffer B + 50 mM NaCl and once with TE (10 mM Tris–HCl, pH 8, 1 mM EDTA). The specifically bound proteins were eluted twice with 0.4 M NaCl and subsequently twice with the Elution buffer (62.5 mM Tris–HCl, pH 6.8, 2% SDS, 10% glycerol, bromophenol blue). In each elution step the beads were incubated with the buffer for 30 min at r.t. in gentle rotation. The eluted proteins from Sample and Control were analyzed by SDS-PAGE and Western blotting using anti-ERp57, anti-APE/Ref-1 (Santa-Cruz), anti-PARP1 and anti-Ku86 antibodies (both from Sigma).

3. Results

3.1 ChIP with anti-ERp57

In vivo protein-DNA cross-linkages were produced in M14 cells with cis-DDP. The DNA-protein complexes were isolated by gel filtration chromatography and subjected to the immunoprecipitation procedure with the anti-ERp57 antibody, as described in section 2.2. The immunoprecipitated DNA was examined by PCR, using the clone-specific primers listed in Table I (Supplementary Material). The enrichment of the DNA fragments in the Sample immunoprecipitation was analyzed in comparison to the unspecific DNA present in the mock immunoprecipitation, where preimmune IgG were used instead of the specific anti-ERp57 antibody. The specificity of the anti-ERp57 antibody purified in our lab has been previously demonstrated [16].

The Fig. 1 (upper panel) shows the results of the PCR amplifications of the various ERp57-interacting DNA regions. The histogram (Fig. 1, bottom panel) represents the semi-quantitative PCR analysis of the enrichment of each ERp57 target region, shown as ratio between the DNA from the Sample immunoprecipitation (S) and the DNA from the mock immunoprecipitation (C). The S/C ratio was obtained from the intensities of the fluorescent DNA bands on agarose gels measured by the Kodak Image Station 2000R. The S/C ratio of the cloned fragments 20, 23, 33, as shown, is less than 1.5, indicating that the specific immunopurified DNA is not significantly enriched.

Among the immunoprecipitated sequences, we selected four clones (listed below) for subsequent analysis, on the basis of the implication of the corresponding genes in the stress response and DNA repair processes:

- Cl 16: intron of *MSH6* (Accession n° NT_022184.15)
- Cl 38: intron of *ETS1* (Accession n° NT_033899.8)
- Cl 42: intron of *LRBA* (Accession n° NT_016354.19)
- Cl 50: 5' region of *TMEM126A* (Accession n° NT_167190.1)

They will be indicated hereafter only with the gene name.

They all exhibited a high *in vivo* affinity for ERp57 in HeLa cells, while the *in vitro* affinity was not confirmed for ETS1 [21].

3.2 ERp57 siRNA silencing

The knockdown of the ERp57 expression was then performed, taking advantage of the RNAi technique. M14 cells were incubated with the specific short interfering RNA (siRNA) for 48 h under their normal growth conditions. The almost complete silencing of the ERp57 protein after the treatment with siRNA has been previously demonstrated by Western blotting analysis of the total M14 cell lysate [10].

The gene silencing was monitored at the mRNA level in order to evaluate if the expression of the ERp57 targeted genes was being affected. Cells treated with scrambled RNA were used as control reference. The expression levels of the ERp57 gene and of its targeted genes were evaluated by Real Time PCR (Fig. 2). In silenced cells, the expression of the MSH6, TMEM126A and LRBA genes was significantly down-modulated, while the ETS1 gene was up-regulated, but this effect resulted not significant. Anova test was used to assess the statistical significance.

3.3 In vitro binding assay

The DNA fragments corresponding to MSH6, TMEM126A, ETS1 or LRBA sequences were amplified with biotinylated primers by PCR and immobilized on streptavidin-coated magnetic beads. In control experiments biotin-saturated streptavidin beads were used. Sample and Control beads were incubated with a nuclear extract from M14 cells, in presence of E. coli DNA in a 500-fold excess as competitor. The bound proteins were eluted using first a high salt concentration (0.4 M NaCl), then 2% SDS, and analyzed by SDS-PAGE and Western blotting with anti-APE/Ref-1, anti-Ku86, and anti-PARP1 antibodies.

As shown in Fig. 3, APE/Ref-1 was found among the proteins of the M14 nuclear extract associated with the regions of the MSH6, TMEM126A, ETS1 and LRBA genes. On the contrary, Ku86 and PARP1 were found both in Sample and Control beads, therefore they probably interacted unspecifically with the biotin-coated streptavidin beads.

3.4 ChIP with anti-APE/Ref-1

In order to verify if APE/Ref-1 was able to bind the aforementioned sequences also *in vivo*, ChIP procedures were performed as described in section 2.2 with an anti-APE/Ref-1 antibody (Sample). Mock experiments (Control) were conducted using IgG from preimmune rabbit serum. The DNA from Sample and Control were analyzed by a standard PCR assay with specific primers (see Table I- Supplementary Material).

Fig. 4 shows the PCR analyses of the enrichment of the DNA regions in the Sample in comparison with the Control. In order to check the efficiency of the immunoprecipitation procedure, the enrichment of the sequence indicated as Ref-1 was analyzed. This is located in the promoter of the Ref-1 gene and is a known APE/Ref-1 binding site [23]. As shown, the sequence in the Ref-1

promoter was immunoprecipitated with the APE/Ref-1 antibody, hence testing the validity of the procedure. The sequence corresponding to the MSH6 sequence resulted a APE/Ref-1 binding site. The S/C value of the cloned fragments ETS1 and TMEM126A is nearly 1, indicating that the specific immunopurified DNA is not significantly enriched. Thus, the ChIP procedure failed to detect the *in vivo* interaction with ETS1 and TMEM126A, although APE/Ref-1 was found associated with them in the *in vitro* binding assays.

4. Discussion and conclusions

A variety of functions have been attributed to ER-resident ERp57, but at the present several questions about the functions of the protein in non ER locations are still unanswered.

The identification of the DNA sequences bound to the nuclear ERp57 has been demonstrated by ChIP procedure on cervical adenocarcinoma cells (HeLa) and the cloning of the immunoprecipitated fragments [21]. The features of these DNA sequences, such as the proximity of MAR regions and the homology to the non-coding regions of orthologue genes of mouse or rat, are compatible with a gene expression regulatory function.

In the present work, ChIP experiments were performed in M14 melanoma cells, where ERp57 binding to the regulatory regions of several STAT3-dependent genes has been already demonstrated [10], investigating the same DNA sequences derived from the double immunoprecipitation and cloning in HeLa cells. As shown in Fig 1, several fragments were confirmed to bind ERp57 with high affinity also in M14 cells.

Among the ERp57-interacting DNA fragments, the genes MSH6, LRBA, ETS1 and TMEM 126A, which code respectively for a DNA mismatch repair protein, the lipopolysaccharide-responsive protein, a transcription factor and potential oncogene, and a recently discovered mitochondrial transmembrane protein, were then subjected to further analyses. The selection has been made on the basis of their high *in vivo* affinity, DNaseI hypersensitivity and the participation of the coded proteins in mostly regulatory processes [21].

The possible regulatory feature of the selected immunoprecipitated fragments has been assessed also in M14 cells. The sequences resulted hypersensitive to DNaseI digestion (data not shown).

Considering the capacity of ERp57 to bind, *in vivo,* specific DNA intronic sequences having the features of regulatory regions, we have supposed that the protein could have a specific function in the nucleus, participating in the control of gene expression. In order to verify this hypothesis, we have exploited a silencing strategy by RNA interference. After a 48 h treatment with the specific siRNA, the expression of ERp57 in M14 cells was markedly reduced. The silencing of endogenous ERp57 produced a significant down-regulation of the MSH6, TMEM126A and LRBA genes, while

the ETS1 gene was up-regulated (Fig. 2); such effect resulted to be not statistically significant, and it can be hypothesized to be due to the treatment itself.

ERp57, like most of the other protein disulfide isomerases, is particularly prone to form complexes with other proteins. ERp57 has been shown to interact with the enhancer of the α2-macroglobulin gene in association with nuclear STAT3 in melanoma cells, where STAT3 is constitutively activated [24]. Moreover, Cicchillitti et al. [25] have detected ERp57 in a nuclear multimeric complex together with proteins involved in cell division and gene expression. In particular, an interaction with nuclear β-actin has been characterized, connected with the resistance to the chemotherapeutic paclitaxel.

Although the *in vitro* affinity of purified ERp57 for DNA has been found to be much lower than that of a typical transcription factor [26], the formation of multiprotein complexes could overcome the scarce propensity to bind to DNA sequences. To verify the involvement of ERp57-containing complexes in transcriptional regulation, we have exploited an *in vitro* binding assay. Biotinylated DNA fragments corresponding to MSH6, TMEM126A, ETS1 or LRBA were immobilized on streptavidin beads and incubated with the M14 nuclear extract. APE/Ref-1, Ku86 and Poly(ADP-ribose) polymerase-1 (PARP1), all involved in the DNA damage response, have been searched in the eluate by Western blotting with specific antibodies. In particular, APE/Ref-1 and the Ku subunits were shown to interact with ERp57 in three human cell lines [19]. The *in vitro* binding assays have shown the interaction of APE/Ref-1 with the ERp57-interacting DNA fragments MSH6, TMEM126A, ETS1 and LRBA (Fig. 3). The binding of Ku86 and PARP1, instead, resulted to be mostly unspecific.

ChIP experiments were also performed to explore the *in vivo* interaction of APE/Ref-1 with the selected DNA fragments (Fig. 4). Only the association with MSH6 has been detected. It can be hypothesized that in the *in vitro* binding assays the presence of APE/Ref-1 among the proteins bound to the immobilized fragments has been due to the association with ERp57, as a consequence of the affinity between the two proteins, and not directly with DNA. Alternatively, APE/Ref-1 can bind directly the DNA fragments but only in *in vitro* conditions and not *in vivo*.

Resuming, ERp57 has been found to directly bind DNA at the level of regulatory regions of genes, several of them involved in the stress response, in three cancer cell lines: HeLa, Raji [21] and M14 cells (as demonstrated in the present work). Furthermore, in our RNAi experiments, the depletion of ERp57 down-modulated the expression of the MSH6, TMEM126A and LRBA genes, leading to the hypothesis of a role in transcriptional regulation. Another member of the protein disulfide isomerases, PDI, has been shown to be involved at the nuclear level in transcriptional regulation, intervening in the activity of the estrogen receptor, by influencing its conformation and modulating its affinity for the estrogen-responsive element [27]. Moreover, recently, an interaction has been

demonstrated between ERp57 and the transcription factor NFkB in leukemia cells and the two proteins were found to translocate towards the nuclear compartment [28].

Among the ERp57-interacting DNA sequences, MSH6 is of particular interest: it is part of the base excission repair machinery and is involved in the DNA mismatch repair in response to DNA alkylating agents. Recently, its induction in response to rapamycin in cis-DDP treated endometrial cancer cells has been demonstrated [29]. Furthermore, both ER stress [30] and mismatch repair proteins [31] have been associated to the pro-apoptotic effect of cisplatin. ChIP assays have also shown the interaction of APE/Ref-1 to MSH6. In concert with several other DNA repair proteins, APE/Ref-1 is part of the base excision repair machinery (BER) of eukaryotic cells [32], and its expression can be up-regulated by a variety of reactive oxygen species (ROS) and ROS-generating systems [33]. Moreover, APE/Ref-1 is a multifunctional protein involved in the regulation of stress inducible transcription factors, such as AP-1, NF-κB, Pax5, Pax8, HIF-1, HLF and of the pro-apoptotic functions of p53 [34]. Interestingly, APE/Ref-1 has been recently found to be required for the DNA binding activity of STAT3 [35].

It can be hypothesized that ERp57, which is known to be over-expressed in a variety of stress conditions [5], could regulate the expression of the MSH6 gene acting as a ER stress sensor, maybe in association with the protein APE/Ref-1.

Acknowledgments

We thank Prof. Anna Ferraro and Prof. Carlo Turano for help in designing the experiments and for critical reading of the manuscript. This work was supported by grants of the Istituto Pasteur-Fondazione Cenci Bolognetti and ‘‘Sapienza’’ Università di Roma. This work was also supported by grants of the ‘‘Enrico ed Enrica Sovena” Foundation Italy.

References

[1] Schrag JD, Procopio DO, Cygler M, Thomas DY, Bergeron JJ (2003) Lectin control of protein folding and sorting in the secretory pathway. Trends Biochem Sci 28:49-57.

[2] Freedman RB, Hirst TR, Tuite MF (1994) Protein disulphide isomerase: Building bridges in protein folding. Trends Biochem Sci 19:331–336.

[3] Li Y, Camacho P (2004) Ca^{2+} dependent redox modulation of SERCA 2b by ERp57. J Cell Biol 164:35-46.

[4] Lindquist JA, Jensen ON, Mann M, Hämmerling GJ (1998) ER-60, a chaperone with thiol-dependent reductase activity involved in MHC class I assembly. EMBO J 17:2186-2195.

[5] Lee A (2001) The glucose-regulated proteins: Stress induction and clinical applications. Trends Biochem Sci 26:504-510.

[6] Hetz C, Russelakis-Carneiro M, Wälchli S, Carboni S, Vial-Knecht E, Maundrell K, Castilla J, Soto C (2005) The disulfide isomerase Grp58 is a protective factor against prion neurotoxicity. J Neurosci 25:2793-2802.

[7] Turano C, Coppari S, Altieri F, Ferraro A (2002) Proteins of the PDI family: Unpredicted non-ER locations and functions. J Cell Physiol 193:154-163.

[8] Turano C, Gaucci E, Grillo C, Chichiarelli S (2011) ERp57/GRP58: a protein with multiple functions. Cell Mol Biol Lett 16:539-563.

[9] Ndubuisi MI, Guo GG, Fried VA, Etlinger JD, Sehgal PB (1999) Cellular physiology of STAT3: Where's the cytoplasmic monomer?. J Biol Chem 274:25499-25509.

[10] Chichiarelli S, Gaucci E, Ferraro A, Grillo C, Altieri F, Cocchiola R, Arcangeli V, Turano C, Eufemi M (2010) Role of ERp57 in the signaling and transcriptional activity of STAT3 in a melanoma cell line. Arch Biochem Biophys 494:178-183.

[11] Sehgal PB, Guo GG, Shah M, Kumar V, Patel K (2002) Cytokine signaling: STATS in plasma membrane rafts. J Biol Chem 277:12067-12074.

[12] Obeid M, Tesniere A, Ghirindelli F, Fimia G, Apetoh L, Perfettini J, Castedo M, Mignon G, Panaretakis T, Casares N, Meivier D, Larochette N, Van Endert P, Ciccosanti F, Piacentini M, Zitvogel L, Kroemer G (2007) Calreticulin exposure dictates the immunogenicity of cancer cell death. Nat Med 13:54-61.

[13] Johnson E, Henzel W, Deisseroth A (1992) An isoform of protein disulfide isomerase isolated from chronic myelogenous leukemia cells alters complex formation between nuclear proteins and regulatory regions of interferon inducible genes. J Biol Chem 267:14412-14417.

[14] Ohtani H, Wakui H, Ishino T, Komatsuda A, Miura B (1993) An isoform of protein disulfide isomerase is expressed in the developing acrosome of spermatids during rat spermiogenesis and is transported into the nucleus of mature spermatids and epididymal spermatozoa. Histochem 100:423-429.

[15] Gerner C, Holzmann K, Meissner M, Gotzmann J, Grimm R, Sauermann G (1999) Reassembling proteins and chaperones in human nuclear matrix protein fractions. J Cell Biochem 74:145-151.

[16] Coppari S, Altieri F, Ferraro A, Chichiarelli S, Eufemi M, Turano C (2002) Nuclear localization and DNA interaction of protein disulfide isomerase ERp57 in mammalian cells. J Cell Biochem 85:325-333.

[17] Markus M, Benezra R (1999) Two isoforms of protein disulfide isomerase alter the dimerization status of E2A proteins by a redox mechanism. J Biol Chem 274:1040-1049.

[18] Krynetski EY, Krynetskaia NF, Bianchi ME, Evans WE (2003) A nuclear protein complex containing high mobility group proteins B1 and B2, heat shock cognate protein 70, ERp60, and glyceraldehyde-3-phosphate dehydrogenase is involved in the cytotoxic response to DNA modified by incorporation of anticancer nucleoside analogues. Cancer Res 63:100-106.

[19] Grillo C, D'Ambrosio C, Scaloni A, Maceroni M, Merluzzi S, Turano C, Altieri F (2006) Cooperative activity of Ref-1/APE and ERp57 in reductive activation of transcription factors. Free Radic Biol Med 41:1113-1123.

[20] Yacoub A, Kelley MR, Deutsch WA (1997) The DNA repair activity of human redox/repair protein APE/Ref-1 is inactivated by phosphorylation. Cancer Res 57:5457-5459.

[21] Chichiarelli S, Ferraro A, Altieri F, Eufemi M, Coppari S, Grillo C, Arcangeli V, Turano C (2007) The stress protein ERp57/GRP58 binds specific DNA sequences in HeLa cells. J Cell Phisiol 210:343-351.

[22] Chichiarelli S, Coppari S, Turano C, Eufemi M, Altieri F, Ferraro A (2002) Immunoprecipitation of DNA-protein complexes cross-linked by cis-diamminedichloroplatinum. Anal Biochem 302:224-229.

[23] Kuninger DT, Izumi T, Papaconstantinou J, Mitra S (2002) Human AP-endonuclease 1 and hnRNP-L interact with a nCaRE-like repressor element in the AP-endonuclease 1 promoter. Nucleic Acids Res 30:823-829.

[24] Eufemi M, Coppari S, Altieri F, Grillo C, Ferraro A, Turano C (2004) ERp57 is present in STAT3-DNA complexes. Biochem Biophys Res Commun 323:1306-1312.

[25] Cicchillitti L, Della Corte A, Di Michele M, Donati MB, Rotilio D, Scambia G (2010) Characterisation of a multimeric protein complex associated with ERp57 within the nucleus in paclitaxel-sensitive and -resistant epithelial ovarian cancer cells: the involvement of specific conformational states of beta-actin. Int J Oncol 37:445-454.

[26] Ferraro A, Altieri F, Coppari S, Eufemi M, Chichiarelli S, Turano C (1999) Binding of the protein disulfide isomerase isoform ERp60 to the nuclear matrix associated regions of DNA. J Cell Biochem 72:528–539.

[27] Schultz-Norton JR, McDonald WH, Yates JR, Nardulli AM. (2006) Protein disulfide isomerase serves as a molecular chaperone to maintain estrogen receptor alpha structure and function. Mol Endocrinol 20:1982-1995.

[28] Wu W, Beilhartz G, Roy Y, Richard CL, Curtin M, Brown L, Cadieux D, Coppolino M, Farach-Carson MC, Nemere I, Meckling KA (2010) Nuclear translocation of the 1,25D3-MARRS (membrane associated rapid response to steroids) receptor protein and NFkappaB in differentiating NB4 leukemia cells. Exp Cell Res 316:1101-1108.

[29] Bae-Jump VL, Zhou C, Boggess JF, Gehrig PA (2009) Synergistic effect of rapamycin and cisplatin in endometrial cancer cells. Cancer 115:3887-3896.

[30] Xu Y, Yu H, Qin H, Kang J, Yu C, Zhong J, Su J, Li H, Sun L (2011) Inhibition of autophagy enhances cisplatin cytotoxicity through endoplasmic reticulum stress in human cervical cancer cells. Cancer Lett doi:10.1016/j.canlet.2011.09.034.

[31] Topping RP, Wilkinson JC, Scarpinato KD (2009) Mismatch repair protein deficiency compromises cisplatin-induced apoptotic signaling. J Biol Chem 284:14029-14039.

[32] Altieri F, Grillo C, Maceroni M, Chichiarelli S (2008) DNA damage and repair: from molecular mechanisms to health implications. Antiox Redox Signal 10:891-937.

[33] Kelley MR, Parsons SH (2001) Redox regulation of the DNA repair function of the human AP endonuclease Ape1/ref-1. Antiox Redox Signal 3:671-683.

[34] Xanthoudakis S, Curran T (1992) Identification and characterization of Ref-1, a nuclear protein that facilitates AP-1 DNA binding activity. EMBO J 11:653-665.

[35] Ray S, Lee C, Hou T, Bhakat KK, Brasier AR (2010) Regulation of signal transducer and activator of transcription 3 enhanceosome formation by apurinic/apyrimidinic endonuclease 1 in hepatic acute phase response. Mol Endocrinol 24:391-401.

Figure legends

Fig. 1 (**Upper panel**) PCR analysis of the enrichment of ERp57 target regions in the immunoprecipitated DNA (S) in comparison with the mock immunoprecipitation (C) in M14 cells. The results correspond to the different cloned regions, listed in Table 1 (Supplementary Material; for clones description see Chichiarelli et al, 2007). The immunoprecipitation was carried out by the use of anti-ERp57 antibody (S) or IgG (C) immobilized on magnetic beads. (**Bottom panel**) Semi-quantitative PCR analysis of the ERp57 target regions enrichment in the immunoprecipitated DNA. The S/C ratio was obtained from the intensities of the fluorescent DNA bands on agarose gels measured by the Kodak Image Station 2000R. The cloned fragments with a S/C ratio less than 1.5 are depicted in grey.

Fig. 2 Effect of ERp57 silencing on the expression of four target genes (MSH6, TMEM126A, LRBA, ETS1). The M14 cells were treated for 48 h with scrambled RNA (control) or siRNA for ERp57 (sil), then total RNA was extracted for the reverse transcriptase Real Time PCR measurement. The gene expression level after ERp57 silencing is here shown relatively to the expression in the control cells, which has been set to 1. The expression of the genes was normalized with that of the housekeeping gene RPS27A. Each value is the average of two experiments ± standard deviation. (*P<0.05).

Fig. 3 Western blotting analysis with the ERp57, APE/Ref-1, Ku86 and PARP1 antibodies, of the proteins specifically bound to the immobilized cloned DNA sequences corresponding to MSH6, ETS1, TMEM126A and LRBA. (C): controls (i.e., proteins from nuclear extract bound to the beads without immobilized DNA). (EN): proteins in the nuclear extract. The proteins were eluted with 0.4 M NaCl and then with 2% SDS.

Fig. 4 (**Left panel**) PCR analysis of the enrichment of APE/Ref-1 target regions in the immunoprecipitated DNA (S) in comparison with the mock immunoprecipitation (C) in M14 cells. The results correspond to the clone regions listed in Table 1 (Supplementary Material; for clones description see Chichiarelli et al, 2007). The immunoprecipitation was carried out with anti-APE/Ref-1 antibody (S) or preimmune rabbit IgG (C) immobilized on magnetic beads. (**Right panel**) Semi-quantitative PCR analysis of the APE/Ref-1 target regions enrichment in the immunoprecipitated DNA. The S/C ratio was obtained from the intensities of the fluorescent DNA bands on agarose gels measured by the Kodak Image Station 2000R.

Fig1
Click here to download high resolution image

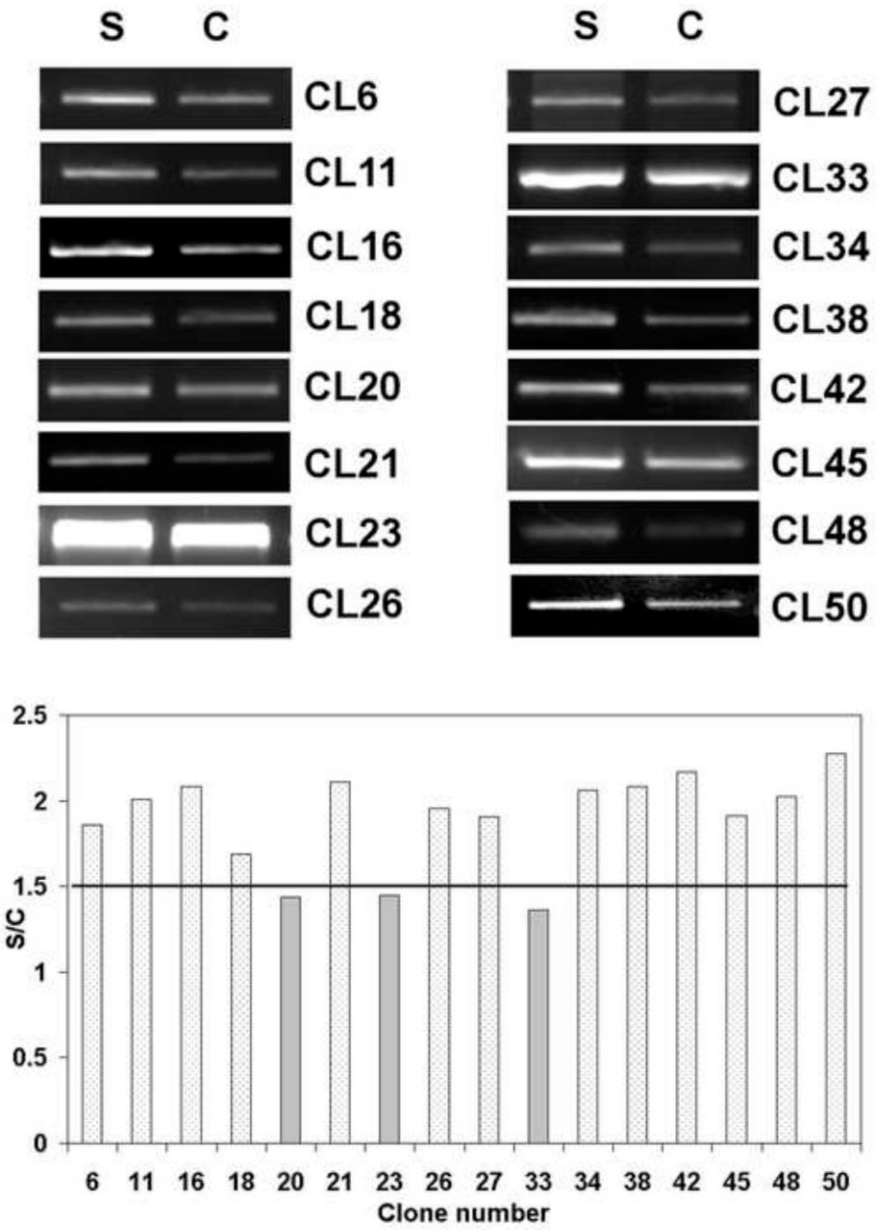

Fig2
Click here to download high resolution image

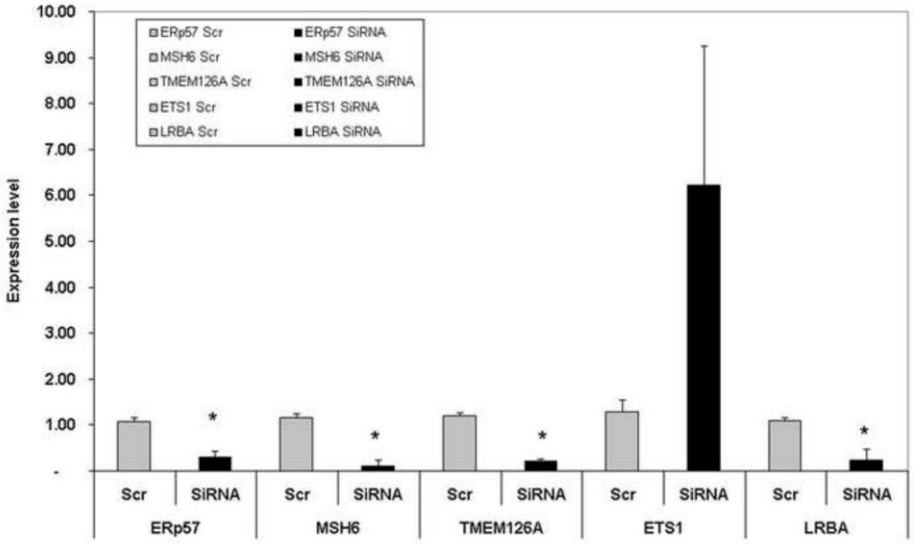

Fig3
Click here to download high resolution image

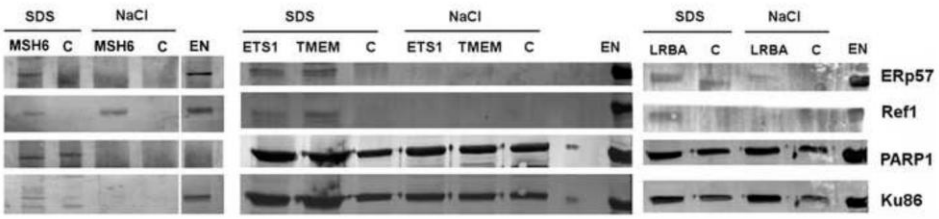

Fig4
Click here to download high resolution image